Cardiomyopathy-associated mutation in the ADP/ATP carrier reveals translation-dependent regulation of cytochrome *c* oxidase activity

Oluwaseun B. Ogunbona, Matthew G. Baile†, and Steven M. Claypool*
Department of Physiology, Johns Hopkins University School of Medicine, Baltimore, MD 21205-2185

ABSTRACT **How the absence of the major mitochondrial ADP/ATP carrier in yeast, Aac2p, results in a specific defect in cytochrome *c* oxidase (COX; complex IV) activity is a long-standing mystery. Aac2p physically associates with respiratory supercomplexes, which include complex IV, raising the possibility that its activity is dependent on its association with Aac2p. Here, we have leveraged a transport-dead pathogenic *AAC2* point mutant to determine the basis for the reduced COX activity in the absence of Aac2p. The steady-state levels of complex IV subunits encoded by the mitochondrial genome are significantly reduced in the absence of Aac2p function, whether its association with respiratory supercomplexes is preserved or not. This diminution in COX amounts is not caused by a reduction in the mitochondrial genome copy number or the steady-state level of its transcripts, and does not reflect a defect in complex IV assembly. Instead, the absence of Aac2p activity, genetically or pharmacologically, results in an aberrant pattern of mitochondrial translation. Interestingly, compared with the complete absence of Aac2p, the complex IV–related defects are greater in mitochondria expressing the transport-inactive Aac2p mutant. Our results highlight a critical role for Aac2p transport in mitochondrial translation whose disturbance uniquely impacts cytochrome *c* oxidase.**

Monitoring Editor
Benjamin S. Glick
University of Chicago

Received: Dec 6, 2017
Revised: Mar 16, 2018
Accepted: Apr 18, 2018

INTRODUCTION

Life is energetically costly. The major energy currency in cells comes in the form of ATP, most of which is produced in the mitochondrion by the combined activities of a series of inner membrane proton pumps (complexes I, III, IV, and V), the last of which physiologically works in reverse. This process, which is known as oxidative phosphorylation (OXPHOS), additionally requires two mitochondrial carrier proteins, the phosphate carrier (Pic) and the ADP/ATP carrier (Aac). A symporter, Pic, couples the downhill flow of protons across the inner membrane to the transport of phosphate into the mitochondrial matrix (Wohlrab and Flowers, 1982). Aac mediates the exchange of ADP into or ATP out of the matrix, a process that is driven by the electrical gradient across the inner membrane that is established by the electron transport chain (Klingenberg, 2008). Thus, Pic and Aac utilize the chemical and electrical components of the electrochemical gradient, respectively, to provide the substrates, Pi and ADP, needed by complex V to make ATP. By reducing the electrochemical gradient, Pic and Aac make it easier for complexes I, III, and IV to pump protons. Further, their transport activity is a core feature of respiratory control, the classic mode of OXPHOS regulation. In the absence of ADP (or Pi), complex V is unable to couple the downhill flow of protons to the synthesis of ATP. This increases the electrochemical gradient to a level that effectively shuts off further proton pumping. Upon the addition of ADP and its transport into the matrix by Aac, complex V function resumes, decreasing the

This article was published online ahead of print in MBoC in Press (http://www.molbiolcell.org/cgi/doi/10.1091/mbc.E17-12-0700) on April 24, 2018.
The authors declare no competing financial interests.

†Present address: Weill Institute for Cell and Molecular Biology and Department of Molecular Biology and Genetics, Cornell University, Ithaca, NY 14853-7202.

O.B.O., M.G.B., and S.M.C. designed and performed the research. O.B.O. and S.M.C. wrote the article, which was edited by M.G.B.

*Address correspondence to: Steven M. Claypool (sclaypo1@jhmi.edu).

Abbreviations used: Aac, ADP/ATP carrier; ANT, adenine nucleotide translocase; BKA, bongkrekic acid; COX, cytochrome *c* oxidase; DDM, *n*-dodecyl β-D-maltoside; EV, empty vector; mtDNA, mitochondrial DNA; OXPHOS, oxidative phosphorylation; Pic, phosphate carrier; TMPD, *N*,*N*,*N*′,*N*′-tetramethyl-*p*-phenylenediamine; WT, wild type.

electrochemical gradient and thus increasing the activity of the respiratory complexes. As such, the OXPHOS machinery, Pic, and Aac are functionally codependent.

In humans, ADP/ATP carriers are called adenine nucleotide translocases (ANT). There are three Aac isoforms in yeast and four ANT isoforms in humans. All of these isoforms are encoded by distinct genes. The four human ANT isoforms display a tissue-specific and yet partially overlapping expression pattern. ANT1 is the predominant isoform in the heart and skeletal muscle (Stepien *et al.*, 1992), ANT2 is highly expressed in regenerative tissues such as kidney and liver, ANT3 is ubiquitously expressed at low baseline levels, and ANT4 is contained in testis (Stepien *et al.*, 1992; Doerner *et al.*, 1997; Dolce *et al.*, 2005; Dupont and Stepien, 2011). Of the three yeast Aac isoforms, only Aac2p is required for OXPHOS (Lawson *et al.*, 1990). Aac1p and Aac3p are minor isoforms whose expression is repressed in hypoxic (Gavurníková *et al.*, 1996) or induced in anaerobic (Sabová *et al.*, 1993) conditions, respectively.

ANT1 deficiency is implicated in various pathological states, such as hypertrophic cardiomyopathy, mitochondrial myopathy, lactic acidosis, progressive external ophthalmoplegia, facioscapulohumeral muscular dystrophy, and Sengers syndrome (Graham *et al.*, 1997; Kaukonen *et al.*, 2000; Jordens *et al.*, 2002; Komaki *et al.*, 2002; Fontanesi *et al.*, 2004; Palmieri *et al.*, 2005; Sharer, 2005; Echaniz-Laguna *et al.*, 2012; Thompson *et al.*, 2016). Mutations in *ANT2* have been associated with nonsyndromic intellectual disability (Vandewalle *et al.*, 2013) and cardiac noncompaction (Kokoszka *et al.*, 2016) and its dysregulation associated with a Warburg metabolic phenotype (Maldonado *et al.*, 2016). Presumably, the impacted tissues reflect the expression pattern of ANT isoforms. However, whether these pathologies all result simply from impaired OXPHOS function or additionally include isoform-specific activities unrelated to OXPHOS remains an open question.

It was demonstrated by us and others that Aac2p physically associates with the respiratory supercomplex (RSC), higher order assemblies of individual respiratory complexes (Schägger and Pfeiffer, 2000; Acín-Pérez *et al.*, 2008; Moreno-Lastres *et al.*, 2012; Gu *et al.*, 2016; Letts *et al.*, 2016; Wu *et al.*, 2016), as well as other mitochondrial carriers, but only in the context of mitochondrial membranes that contain the unique phospholipid cardiolipin (Claypool *et al.*, 2008; Dienhart and Stuart, 2008). Importantly, we have recently established that the interaction between the ADP/ATP carrier and the respiratory supercomplexes is evolutionarily conserved (Lu *et al.*, 2017), implying that this association is functionally important. However, the functional significance of the Aac2p interaction with respiratory supercomplexes has not been provided.

The absence of Aac2p in yeast not only prevents OXPHOS but additionally results in a specific diminution in complex IV activity (Heidkämper *et al.*, 1996; Müller *et al.*, 1996; Fontanesi *et al.*, 2004; Claypool *et al.*, 2008; Dienhart and Stuart, 2008). The mechanistic basis for the reduced complex IV function when Aac2p is missing has not been established. In the present study, we have modeled a transport-dead pathogenic *ANT1* point mutant discovered in a patient with hypertrophic cardiomyopathy and mild myopathy in *AAC2* to determine whether the reduction in complex IV activity when Aac2p is missing reflects the absence of the interaction between Aac2p and components of the electron transport chain and/or the lack of nucleotide transport (i.e., Aac2p function). Importantly, the functionally inactive A137D allele of *AAC2* (*aac2*^{A137D}) is expressed normally and still interacts with components of the yeast respiratory supercomplex. In the absence of Aac2p function, the expression levels of complex IV subunits that are encoded by the mitochondrial genome (and which form the catalytic core of the complex IV holoenzyme) are specifically reduced. This reduction in the levels of complex IV subunits is not caused by a decrease in mitochondrial genome copy number or levels of mitochondrial DNA (mtDNA) transcripts, nor does it result from any alteration in complex IV assembly. Instead, mitochondrial translation is altered in the absence of Aac2p activity. Interestingly, compared with the complete absence of Aac2p, the complex IV–related defects are greater in mitochondria expressing the transport-inactive Aac2^{A137D}. Collectively, our results highlight the importance of Aac2p function for the normal translation of the mitochondrial encoded complex IV subunits and further underscore the significant role of Aac2p in regulating oxidative phosphorylation.

RESULTS

Aac2^{A137D} is nonfunctional but assembles like wild-type Aac2p

In yeast, complex IV function is specifically impaired in the absence of Aac2p. Even though this was first documented more than two decades ago (Heidkämper *et al.*, 1996; Müller *et al.*, 1996) and subsequently confirmed by multiple groups (Fontanesi *et al.*, 2004; Claypool *et al.*, 2008; Dienhart and Stuart, 2008), the underlying mechanism has never been provided. In principle, Aac2p could support full complex IV activity by either mediating the flux of ADP and ATP across the inner membrane (Heidkämper *et al.*, 1996) and/or by virtue of its physical association with the respiratory supercomplexes (Claypool *et al.*, 2008; Dienhart and Stuart, 2008). To distinguish between these possibilities, we decided to leverage a pathogenic allele of ANT1, ANT1^{A123D}, identified in a patient suffering from exercise intolerance, lactic acidosis, hypertrophic cardiomyopathy, and mild myopathy (Palmieri *et al.*, 2005). Interestingly, although the mutant protein is expressed at normal levels, it fails to mediate uptake of ATP upon reconstitution of muscle-derived mitochondrial extracts into liposomes. Moreover, when modeled in the yeast orthologue, Aac2^{A137D} is expressed at wild-type (WT) levels, lacks ADP/ATP exchange in reconstituted liposomes, and fails to support respiratory growth (Palmieri *et al.*, 2005). However, the quaternary assembly of Aac2^{A137D} has not been documented. We reasoned that if Aac2^{A137D} retains its ability to interact with other proteins, including the RSCs, it would provide an ideal tool to determine exactly how Aac2p controls complex IV activity.

Using CRISPR-Cas9, genomic mutations were introduced in *AAC2* that either resulted in a premature stop codon (*aac2*Δ) or the expression of the *aac2*^{A137D} mutant allele (Figure 1A). These genetic modifications were introduced in the presence or absence of Aac1p and Aac3p, to evaluate whether the minor Aac isoforms could potentially compensate for the absence of Aac2p function. As anticipated (Palmieri *et al.*, 2005), Aac2^{A137D} was expressed like WT Aac2p but unable to support growth on respiratory media (Figure 1, A and B). Next, Aac2^{A137D} assembly was compared with WT Aac2p by blue native (BN)–PAGE (Figure 1C). Indeed, Aac2^{A137D} engaged in a normal range of complexes that were not influenced by the presence or absence of the minor Aac isoforms. Importantly, the Aac2^{A137D} -containing complexes included high molecular weight associations with respiratory supercomplexes that consist of a complex III dimer associated with one to two copies of complex IV. In the absence of Aac2p function (*aac2*Δ and *aac2*^{A137D}), the relative abundance of the small supercomplex (III_2IV) was increased and free complex III dimers were readily detected (Figure 1, D and E). These alterations suggest that the steady-state level of complex IV is perhaps limiting when Aac2p is nonfunctional. To directly determine the ability of Aac2^{A137D} to associate with respiratory supercomplexes, we established yeast strains in which a FLAG tag was genomically appended

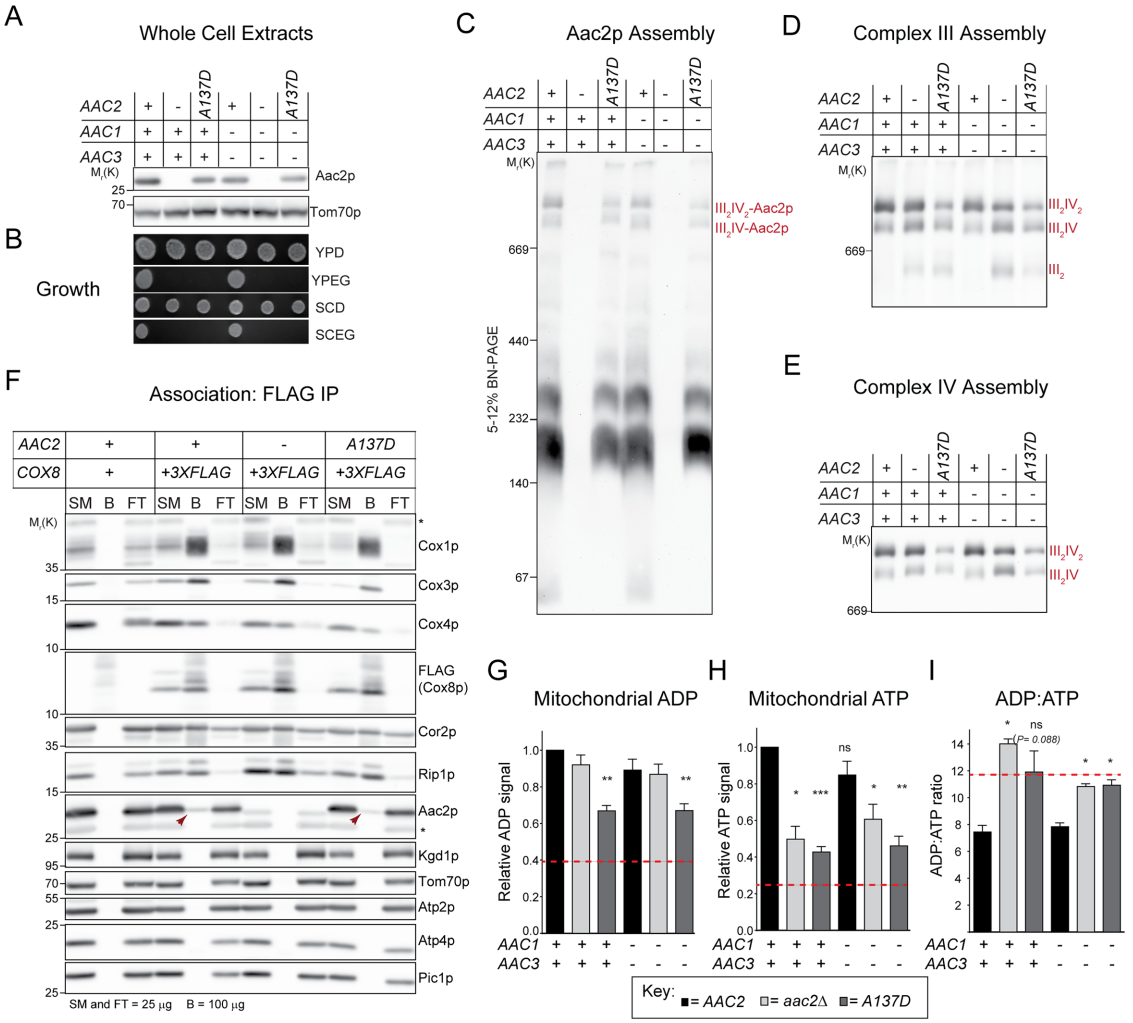

FIGURE 1: A nonfunctional Aac2p mutant is expressed and assembled normally. (A) Whole cell extracts from the indicated yeast strains were resolved by SDS–PAGE and immunoblotted for Aac2p. (B) Growth of the indicated strains on dextrose or ethanol–glycerol media at 30°C for 3 d. $n = 3$. (C–E) Mitochondria (50 µg protein) solubilized in 1.5% (wt/vol) digitonin were resolved by 5–12% 1D Blue Native (BN)–PAGE and (C) Aac2p, (D) complex III (Rip1p), and (E) complex IV (Cox4p) detected by immunoblot. $n = 3$. (F) Following solubilization with 1.5% (wt/vol) digitonin, anti-FLAG resin was used to immunoprecipitate Cox8-3XFLAG (subunit of complex IV) and the presence of copurified respiratory supercomplex subunits determined by immunoblot; Kgd1p and Tom70p served as controls. SM, starting material; B, bound material; FT, nonbinding flow through. $n = 3$. *, nonspecific bands. (G) ADP and (H) ATP levels in mitochondria. Luminescence values relative to wild type are shown. (I) Calculated mitochondrial ADP:ATP ratios. Mean ± SEM, $n = 4$. Statistical difference relative to wild type is shown. The red dotted line refers to the values in a strain lacking mtDNA (rho null).

to the C-terminus of either the complex IV subunit, Cox8p, or the complex III subunit, Qcr10p (Supplemental Figure S1). Indeed, Aac2^{A137D} was coimmunoprecipitated with either Cox8-3XFLAG (Figure 1F) or Qcr10-3XFLAG (Supplemental Figure S1A). Finally, the levels of ADP and ATP in mitochondria were determined as a proxy of Aac2^{A137D} function. In the absence of Aac2p activity, the level of mitochondrial ATP was significantly reduced (Figure 1H), which resulted in an elevated ADP:ATP ratio (Figure 1I). Interestingly, ADP levels were only significantly decreased for *aac2*^{A137D} and not *aac2*Δ (Figure 1G). Combined, these results indicate that Aac2^{A137D} is an assembly-competent, transport-inactive molecular tool that can be used to probe the molecular basis for the reduced complex IV activity that occurs when Aac2p is not expressed (Heidkämper *et al.*, 1996; Müller *et al.*, 1996; Fontanesi *et al.*, 2004; Claypool *et al.*, 2008; Dienhart and Stuart, 2008).

Impaired complex IV activity and expression in the absence of Aac2p function

With the goal of determining whether complex IV activity is dependent on its physical association with Aac2p, we next compared complex IV function in mitochondria that express either transport-active Aac2p, the transport-inactive Aac2^{A137D}, or that lack Aac2p expression completely. To determine complex IV activity in isolation, the rate of cytochrome *c* oxidation was tracked spectrophotometrically using mitochondria solubilized with *n*-dodecyl β-d-maltoside (DDM), a detergent that separates respiratory supercomplexes into its individual components (Schägger, 2001; Figure 2A). To assess complex IV function in intact, nondetergent solubilized mitochondria, the ascorbate-TMPD (*N*,*N*,*N*′,*N*′-tetramethyl-*p*-phenylenediamine)–dependent basal and uncoupled respiration rates, the only measurements that are relevant in the absence of Aac2p function, were

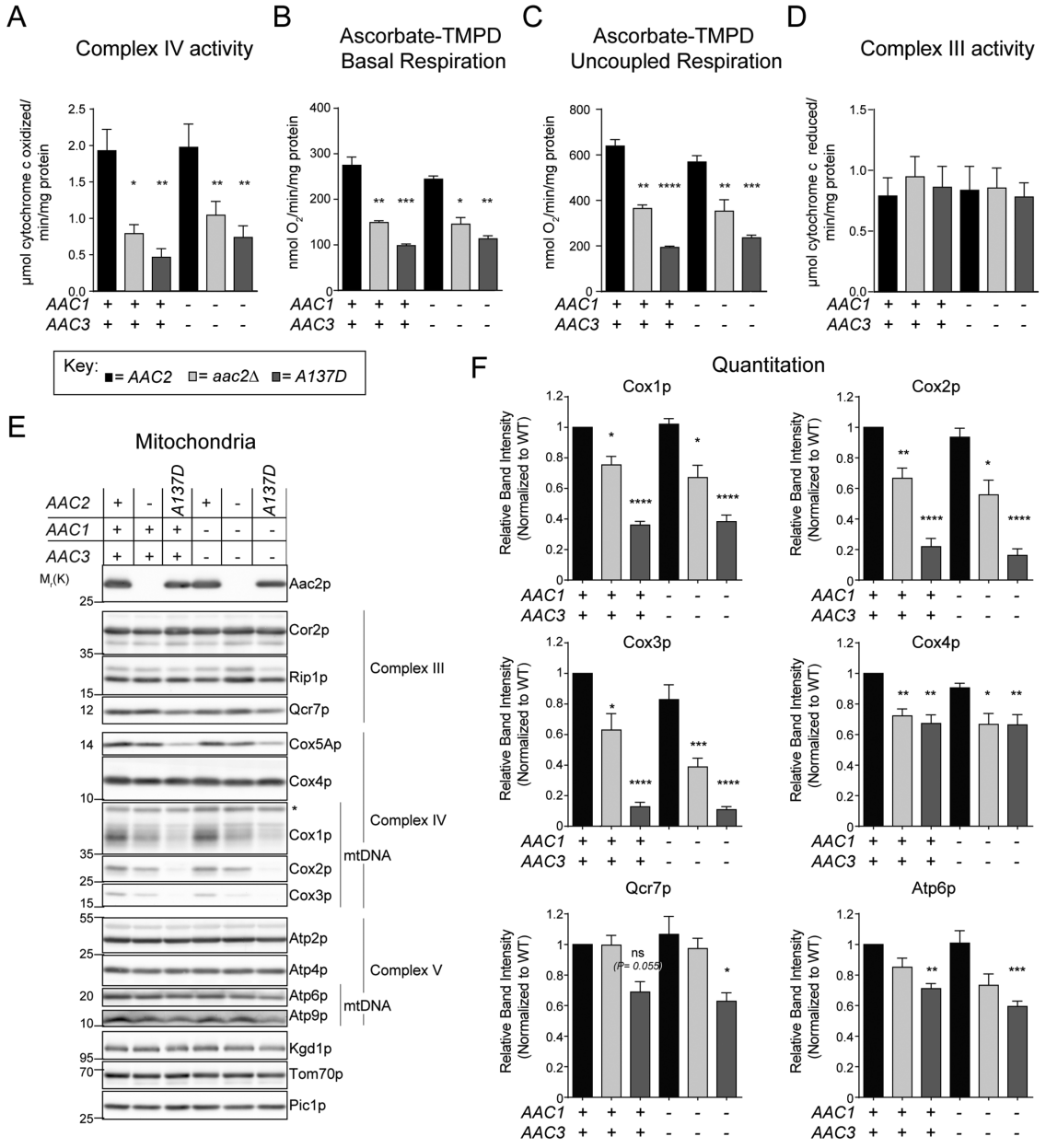

FIGURE 2: Oxidative phosphorylation is impaired in the absence of Aac2p function. (A) Spectrophotometric measurement of complex IV activity in DDM-solubilized mitochondria. Mean ± SEM, $n = 6$. (B) Basal and (C) uncoupled respiration (+CCCP) in intact mitochondria using ascorbate + TMPD (donate electrons to complex IV) as substrate. Mean ± SEM, $n = 6$. (D) Spectrophotometric measurement of complex III activity in DDM-solubilized mitochondria. Mean ± SEM, $n = 6$. (E) Mitochondrial extracts were resolved by SDS–PAGE and immunoblotted for various mitochondrial proteins—Kgd1p (matrix), Tom70p (outer membrane), Atp2p/Atp4p/Atp6p/Atp9p (Complex V), Pic1p (phosphate carrier), Cor2p/Rip1p/Qcr7p (complex III), Cox1-4p/Cox5Ap (complex IV), and Aac2p; *, nonspecific band. (F) Steady-state levels of Cox1-4p, Qcr7p, and Atp6p relative to WT were quantified. Mean ± SEM, $n \geq 4$. Statistical difference relative to wild type is shown for significant comparisons.

determined (Figure 2, B and C). Regardless of the method, complex IV (Figure 2, A–C), but not complex III (Figure 2D), activity was significantly reduced in mitochondria that lack Aac2p function. Interestingly, the level of complex IV activity supported by the transport-inactive Aac2^{A137D} was even lower than detected in *aac2*Δ (Figure 2, A–C). Thus, the reduced complex IV activity in *aac2*Δ extracts stems from the absence of Aac2p–mediated ADP/ATP exchange and not from the lack of the Aac2p–respiratory supercomplex interaction.

Next, the relative abundance of various complex IV subunits was determined in isolated mitochondria (Figure 2E). In yeast, complex IV has 11 total subunits, three of which—Cox1p, Cox2p, and Cox3p—are encoded by the mitochondrial genome. The steady-state levels of all three mtDNA-encoded complex IV subunits was significantly reduced in the absence of Aac2p function (Figure 2E; quantified in Figure 2F and Supplemental Figure S2). This impacted the abundance of other complex IV subunits encoded by the nuclear genome such as Cox5Ap and Cox4p. mtDNA-encoded subunits of complex V (Atp6p and Atp9p) were also reduced when Aac2p activity is missing, although not as drastically as the complex IV subunits. The steady-state amounts of nuclear-encoded subunits

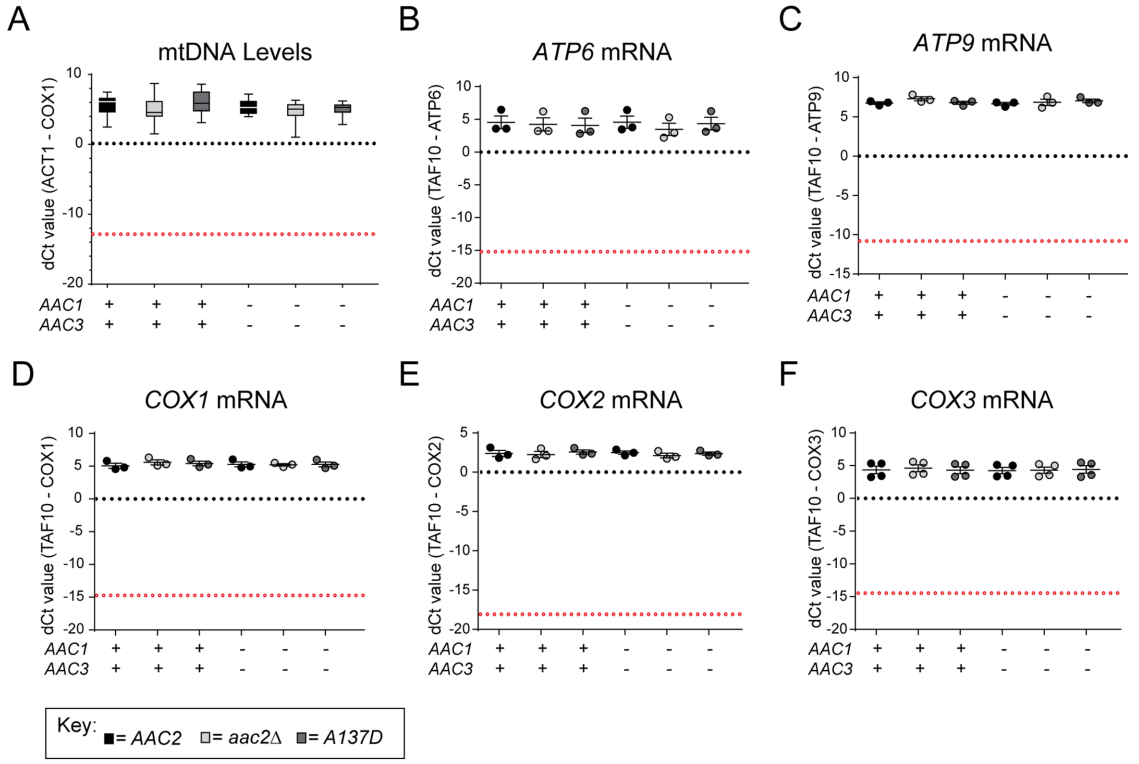

FIGURE 3: The regulation of mitochondrial genome encoded subunits of cytochrome *c* oxidase by Aac2p activity is posttranscriptional. (A) Boxplots showing mtDNA level in the indicated strains determined by quantitative PCR (qPCR) of *COX1* in mtDNA and normalized to *ACT1* in the nucleus. Whiskers represent 5th and 95th percentiles. $n = 12$. (B–F) Interleaved scatterplot showing the steady-state transcript levels of mtDNA-encoded subunits determined by two-step reverse transcription-quantitative PCR for complex IV (*COX1-3*) and complex V (*ATP6, ATP9*) subunits. *TAF10* is a nuclear-encoded reference gene. $n \geq 3$. The red dotted line refers to the calculated dCt values in a strain lacking mtDNA (rho null).

of complex III (except for Qcr7p, which was affected in the *aac2*^{A137D} mutant but not in *aac2*Δ) and complex V, as well as markers of the outer membrane, inner membrane, and matrix compartments (Tom70p, Pic1p, and Kgd1p, respectively), were not altered when Aac2p was absent or nonfunctional. The relative decrease in steady-state abundance of mtDNA-encoded complex IV subunits was roughly proportional to the reduction in complex IV activity observed in mitochondria when Aac2p was not expressed at all (25–61% decrease in expression vs. 43–59% decrease in activity). Similarly, complex IV activity was compromised proportionately to its expression, although to a greater extent in the transport-inactive *aac2*^{A137D} mutant (62–89% decrease in expression vs. 59–76% decrease in activity). This suggests that it is more detrimental to express a nonfunctional version of Aac2p than to not express it at all. From these results, we conclude that Aac2p activity controls complex IV functionality by specifically affecting the levels of mtDNA-encoded subunits of cytochrome *c* oxidase.

Mitochondrial translation is altered in the absence of Aac2p function

The steady-state level of a protein is dictated by how robustly it is produced combined with how stable it is once it is made. Therefore, to determine the basis for the reduced steady-state levels of mtDNA-encoded complex IV subunits, we started at the genetic source of these subunits and determined mtDNA copy number relative to the nuclear genome by qPCR. Consistent with the fact that *aac2*Δ yeast are so-called petite-negative (i.e., yeast lacking Aac2p are unable to survive in the absence of the mtDNA; Kovác *et al.*, 1967), mtDNA copy number was not significantly altered in strains lacking Aac2p activity compared with strains that have Aac2p activity (Figure 3A). We next reasoned that a specific reduction in the levels of complex IV subunits encoded by mtDNA could stem from a defect in their transcription. However, the relative abundance of transcripts that encode for subunits of complex IV (*COX1-3*) or complex V (*ATP6* and *ATP9*) were not impacted by the presence or absence of Aac2p function (Figure 3, B–F).

These results suggest that Aac2p function regulates the steady-state accumulation of mtDNA-encoded complex IV subunits through a posttranscriptional mechanism(s). As such, the translation of mtDNA-encoded proteins was determined by tracking the incorporation of ^{35}S-Met/Cys in yeast cultured in the presence of cycloheximide to inhibit cytosolic translation (Figure 4A and Supplemental Figure S3A). In the absence of Aac2p activity, translation of Cox1p and Cox2p was reduced while curiously, translation of Atp6p and Atp9p was increased relative to Aac2p-expressing yeast (Figure 4A and Supplemental Figure S3A). The latter change resulted in a significantly reduced ratio of newly translated Cox3p to Atp6p in yeast devoid of Aac2p activity (Figure 4B). Translation of Var1p was similar among the different yeast strains (Supplemental Figure S3B), and while the overall incorporation of ^{35}S-Met/Cys was greatest when Aac2p was not expressed, this was not statistically significant (Supplemental Figure S3C). Next, pulse-chase experiments were performed to determine whether the absence of Aac2p function altered the stability of newly translated mtDNA-encoded polypeptides (Figure 4C). In the absence, but not the presence, of the minor Aac isoforms, the stability of Cox1p and Cox2p was compromised in the

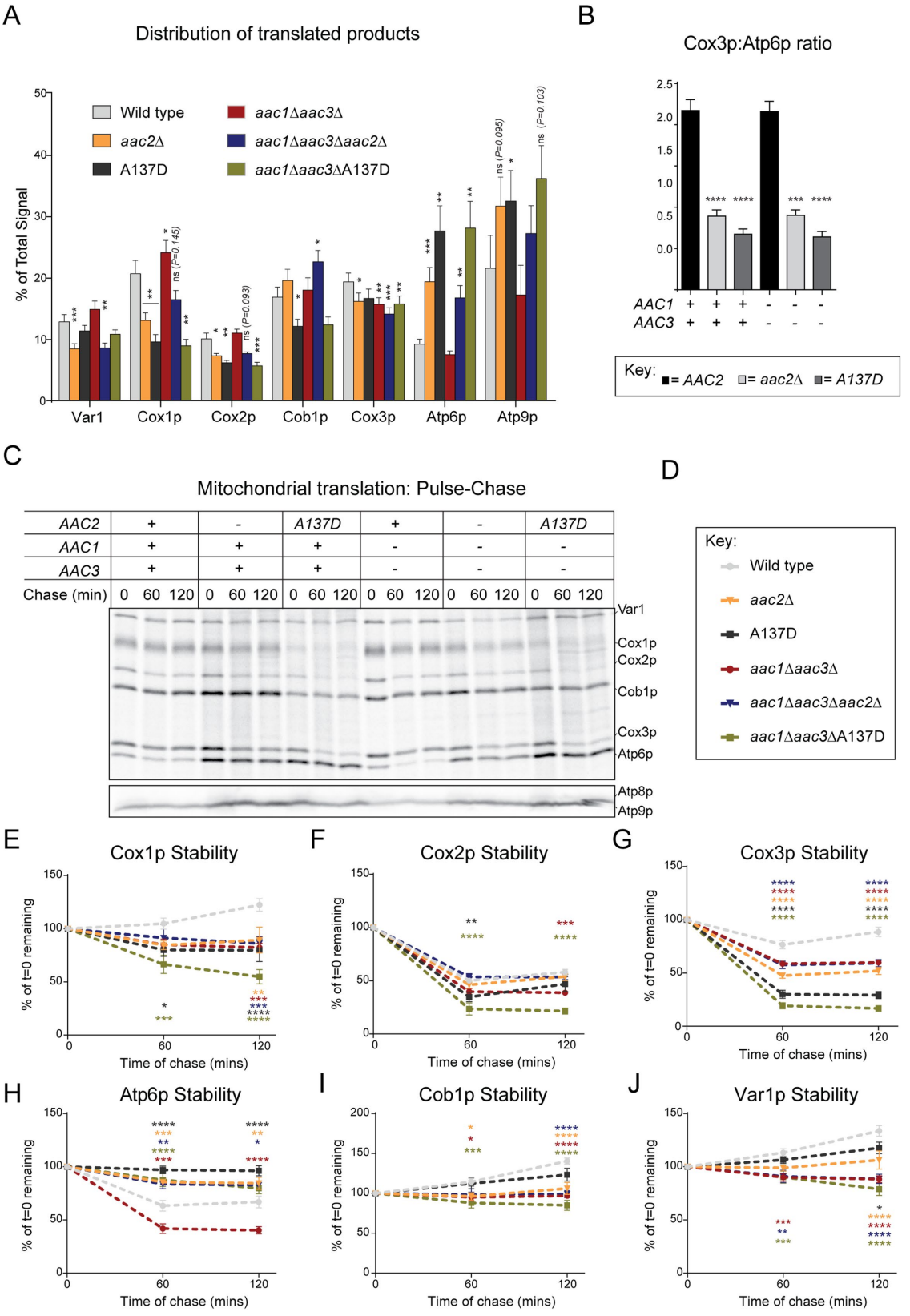

FIGURE 4: Aberrant mitochondrial translation in the absence of Aac2p function. (A) Yeast cultures were spiked with 62 µCi/ml ^{35}S-Met/Cys and **0.2** mg/ml cycloheximide to inhibit cytosolic translation. After 10 and 20 min incubation at 30°C, extracts were harvested, resolved by 12–16% SDS–PAGE (Supplemental Figure S3A), and bands identified by phosphoimaging. The distribution of signals from all the mitochondrial encoded translated proteins is expressed as a percentage of the total signal for each experiment. Mean ± SEM, $n = 10$ for everything (this includes the $t = 0$ timepoints presented in the pulse-chase experiments in C), except Atp9p; $n = 5$). Only statistically significant comparisons relative

context of the transport-inactive Aac2^{A137D} mutant (Figure 4, E and F). However, because the steady-state levels of Cox1p and Cox2p were similarly decreased in Aac2^{A137D} mitochondria with or without the minor Aac isoforms (Figure 3), it is unlikely that the stability of newly translated Cox1p and Cox2p significantly contributes to their reduced steady-state levels. Instead, their translation appears to correlate more strongly with their final steady-state abundance. In contrast, the stability of freshly translated Cox3p was decreased in Aac2^{A137D} mitochondria regardless of the presence of the minor Aac isoforms (Figure 4G). Surprisingly, the stability of newly translated Atp6p was increased when Aac2p function was lacking (Figure 4H). An increased translation of Atp6p (Figure 4A) combined with an enhanced stability of newly made polypeptide (Figure 4H) would be expected to result in increased steady-state Atp6p levels, something that was not observed (Figure 2). Finally, in the presence, but not the absence, of the minor Aac isoforms, the turnover of Cob1p and Var1p was modestly but significantly increased when Aac2p is missing (*aac2*Δ; Figure 4, I and J).

Overall, our results indicate that when Aac2p function is absent, mitochondrial translation is dysregulated such that the production of the complex IV subunits Cox1p and Cox2p, and the complex V subunits Atp6p and Atp9p, is decreased and increased, respectively. Further, our data suggest that the relatively lower steady-state levels of mtDNA-encoded complex IV subunits in *aac2*^{A137D} versus *aac2*Δ mitochondria (Figure 3) may stem in part from a reduced stability of newly translated Cox3p in the former (Figure 4G).

Import and assembly of nuclear-encoded subunits of cytochrome *c* oxidase is not disturbed in the absence of Aac2p function

The assembly of complexes III, IV, and V in yeast involves the coordinated incorporation of proteins from two genomes, and for the two respiratory complexes, the complement of prosthetic groups that endow them with the ability to move electrons. Current evidence suggests that the three mtDNA-encoded COX subunits form three independent modules of distinct composition (McStay *et al.*, 2013a,b; Su *et al.*, 2014). The assembly of these modules is closely monitored and tightly regulated. For example, Mss51p is a Cox1p translational activator that additionally functions as a chaperone that physically stabilizes nascent Cox1p (Siep *et al.*, 2000; Barrientos *et al.*, 2002; Perez-Martinez *et al.*, 2003; Mick *et al.*, 2010). When functioning as a chaperone, Mss51p is unable to act as a Cox1p translational enhancer. As such, Cox1p synthesis is directly linked to the fidelity of its assembly. The complex IV holoenzyme is generated by the association of the three fully assembled modules and any remaining subunits.

Because a defect in complex IV assembly can negatively feedback to reduce mitochondrial translation of complex IV subunits (Perez-Martinez *et al.*, 2003; Barrientos *et al.*, 2004; Towpik, 2005; Soto *et al.*, 2012), we reasoned that Aac2p function may be specifically important for the assembly of complex IV. To test this model, we compared the incorporation of newly imported subunits into complex IV and complex IV–containing supercomplexes in mitochondria that contain or lack Aac2p activity (Brandner *et al.*, 2005). To monitor multiple stages of complex IV assembly, we followed the import and assembly of radiolabeled Cox5Ap and Cox13p, which are integrated into the Cox1p (McStay *et al.*, 2013a,b) and Cox3p (Su *et al.*, 2014) modules, respectively (Figure 5A). Both precursors were imported into isolated mitochondria in a time- and membrane potential–dependent manner regardless of the presence or absence of Aac2p function (Figure 5, B and C). Further, their incorporation into complex IV and complex IV–containing respiratory supercomplexes was not impacted by the absence of Aac2p transport (Figure 5, D and E). Interestingly, the incorporation of radiolabeled Cox5Ap into complex IV–containing complexes was increased in *aac2*Δ mitochondria compared with mitochondria expressing either transport-active or transport-inactive Aac2p. Although the basis for this observation is presently unclear, it is unlikely to reflect reduced steady-state levels of Cox5Ap, which were normal in *aac2*Δ mitochondria (Figure 2E).

Altered mitochondrial translation in the absence of Aac2p function is reversible

Mss51p, a specific translational activator of *COX1* mRNA, is involved in complex IV biogenesis by regulating the synthesis of Cox1p (Siep *et al.*, 2000). When Mss51p is trapped in a complex consisting of unassembled Cox1p and other proteins, it is prevented from enhancing Cox1p translation (Perez-Martinez *et al.*, 2003, 2009; Barrientos *et al.*, 2004; Fontanesi *et al.*, 2011). Unlike its translational target and subsequent client Cox1p, Mss51p accumulated normally in the absence of Aac2p activity (Figure 6A). Next, the ability of overexpressed Mss51p to rescue mitochondrial protein synthesis in the absence of Aac2p function was determined (Figure 6B). However, mitochondrial translation was not altered when Mss51p was overexpressed regardless of the presence or absence of Aac2p function (Figure 6B and Supplemental Figure S4A). These results indicate that the availability of Mss51p to serve as a *COX1* translational activator is not limiting in the absence of Aac2p activity. As such, the reduced translation of complex IV subunits that occurs when Aac2p function is missing does not derive from any changes in Mss51p expression and function.

Aim23p or mIF3p (mitochondrial translation initiation factor 3), the *Saccharomyces cerevisiae* homologue of the bacterial translation initiation factor 3 (IF3), has conserved and overlapping functions with human mIF3p (Atkinson *et al.*, 2012; Kuzmenko *et al.*, 2014). Translation initiation factors act at a critical point between the first (translation initiation) and last (ribosomal recycling) steps of the translational cycle, ensuring correct tRNA and mRNA selection; however, unlike translational activators, translation initiation factors do not directly interact with mRNAs (Kuzmenko *et al.*, 2014). Aim23p disruption results in disturbed mitochondrial translation (Kuzmenko *et al.*, 2016), similar to what we have observed in the absence of Aac2p function (Figure 3). As such, we investigated whether Aim23p is involved in the abnormal mitochondrial translation detected in absence of Aac2p function. However, not only was its steady-state abundance normal in the absence of Aac2p activity (Figure 6C), overexpression of Aim23p failed to improve the Aac2p-related

to WT are displayed. (B) The ratio of Cox3p to Atp6p signals was quantitated. Mean ± SEM, $n = 10$. (C) After 20 min of pulse, 4 μg/ml puromycin and 24.2 μM cold Met/Cys were added and samples collected at $t = 0$ and after 60 and 120 min of chase. Extracts were resolved on 17.5% (top) and 12–16% (bottom) SDS–PAGE, and bands identified by phosphoimaging. $n = 5$. (D) Key for quantitations presented in E–J. The relative signal for mitochondrial translated products in the pulse-chase experiment was quantified taking the signal at $t = 0$ as 100%. Mean ± SEM, $n = 5$. Significant differences of the percent remaining at $t = 60$ and 120 min relative to wild type are shown.

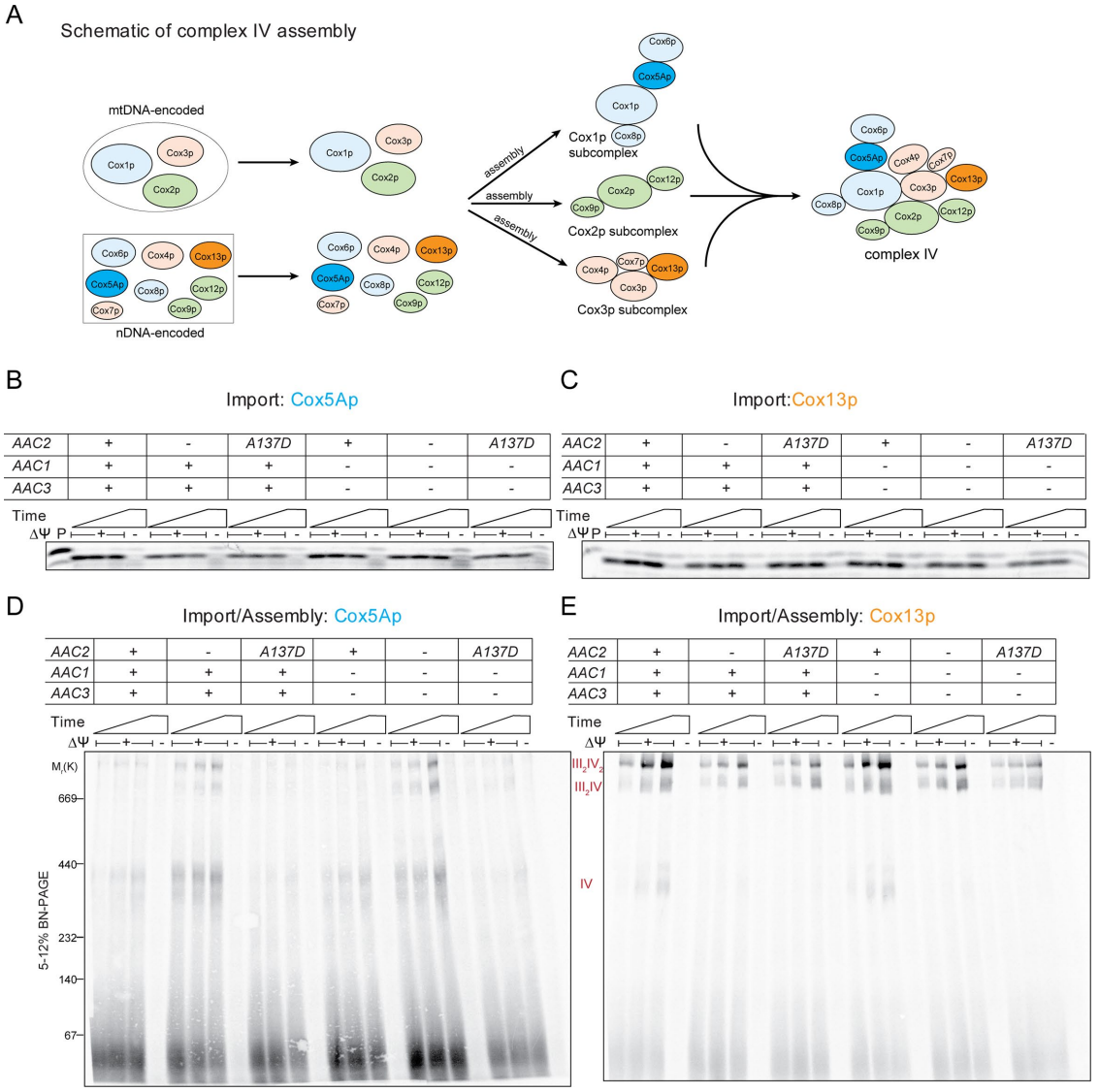

FIGURE 5: Assembly of cytochrome *c* oxidase is not impaired in the absence of Aac2p function. (A) Schematic of complex IV assembly (McStay *et al.*, 2013a,b; Su *et al.*, 2014). An early assembly intermediate centered around Cox1p contains Cox5Ap. Cox13p is incorporated in the Cox3p-assembly module that is added later in the assembly process. Radiolabeled Cox5Ap (B, D) or Cox13p (C, E) was incubated with mitochondria from the indicated strains at 30°C and in the presence (+ΔΨ) or absence (–ΔΨ) of the electrochemical gradient across the inner membrane. Following incubation for 5, 15, or 45 min, nonimported precursors were removed with trypsin and the recovered mitochondria were resolved by 15% SDS–PAGE to monitor import (B, C) or solubilized in 1% (wt/vol) digitonin and resolved by BN–PAGE (D, E) to follow assembly postimport. Bands were identified by phosphoimaging. $n = 3$. P, precursor (5% of each timepoint).

mitochondrial translation defect (Figure 6D and Supplemental Figure S4B). Thus, it would appear that the altered mitochondrial translation in the absence of Aim23p or Aac2p is mechanistically unrelated.

As a control, we determined the ability of overexpressed WT Aac2p to rescue the translational impairment that occurs when Aac2p function is absent. As expected, reintroduction of Aac2p increased the translation of mitochondrial encoded subunits of complex IV (Figure 6, B and D) and restored their steady-state amounts (Supplemental Figure S4C) in both *aac2*Δ and *aac2*^{A137D} yeast.

Acute Aac2p inhibition alters mitochondrial translation

To gain further insight into how Aac2p function promotes normal mitochondrial translation, we asked whether acute inhibition of Aac2p activity using the membrane permeable Aac2p inhibitor, bongkrekic acid (BKA), could prevent the rescued translation of complex IV subunits provided by overexpressed WT Aac2p. Indeed, the increased translation of complex IV subunits was prevented by the inclusion of BKA in the context of either *aac2*^{A137D} rescued with overexpressed Aac2p (Figure 7, A and B) or the WT strain with endogenous or overexpressed Aac2p (Figure 7, C and D). Because this effect occurred after only 10 min of Aac2p inhibition, this suggests that the altered mitochondrial translation detected upon genetic inactivation of Aac2p function does not stem from compensatory processes and instead reflects a direct functional link between Aac2p-mediated transport and normal mitochondrial translation.

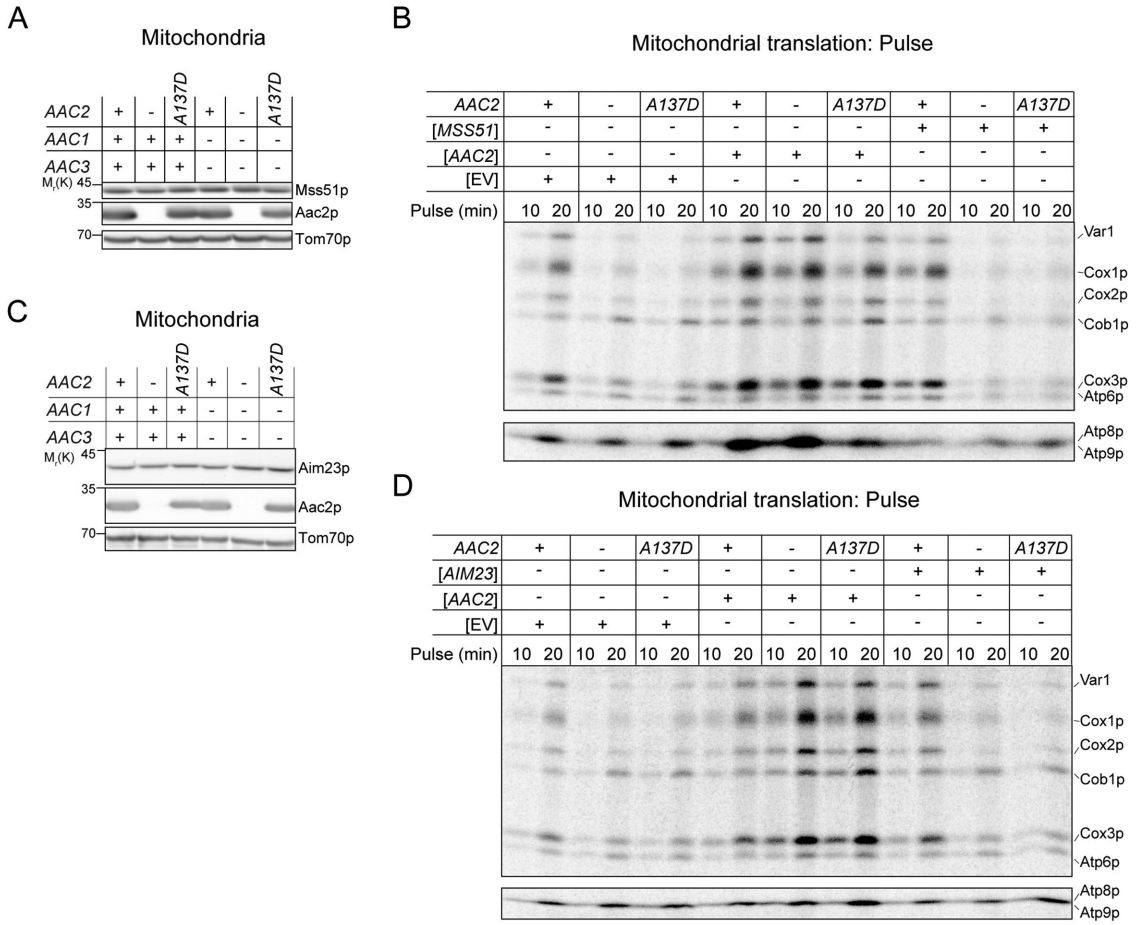

FIGURE 6: Alteration of mitochondrial translation is rescued by overexpression of Aac2p. (A) Mitochondrial extracts (50 µg) were resolved by SDS–PAGE and immunoblotted for Mss51p (translational activator for the *COX1* mRNA) and Aac2p. $n = 6$. (B) Mitochondrial translation was performed as in Figure 4. After 10 and 20 min incubation at 30°C, extracts were harvested, resolved by 17.5% SDS–PAGE, and bands identified by phosphoimaging. EV, empty vector. $n = 3$. (C) Mitochondrial extracts (50 µg) were resolved by SDS–PAGE and immunoblotted for Aim23p (mitochondrial translation initiation factor) and Aac2p. $n = 4$. (D) Mitochondrial translation after 10 and 20 min incubation. Following resolution by 17.5% SDS–PAGE, bands were identified by phosphoimaging. $n = 3$.

Acute Aac2p inhibition reduces the stability of nascent Cox3p

The stability of nascent Cox3p was specifically decreased in Aac2^{A137D} mitochondria (Figure 4G). Because inhibition of WT Aac2p with BKA results in a protein that is expressed but nonfunctional, similar to Aac2^{A137D}, we determined whether acute Aac2p inhibition also increases the turnover of newly translated Cox3p. We initially performed a series of experiments using *aac2*^{A137D} rescued with overexpressed Aac2p, with EV–transformed WT and *aac2*^{A137D} yeast serving as controls (Supplemental Figure S5). Surprisingly, the stability of Cox3p was unaffected by BKA in any of the tested strains (Supplemental Figure S5E). However, the turnover of Cox3p was notably different in untransformed (Figure 4G) versus empty vector (EV)–transformed WT yeast (Supplemental Figure S5E). To determine whether these discrepant results stem from the different media employed (e.g., rich media vs. minimal auxotrophic selection media), we compared WT and *aac2*^{A137D} strains with/without EV, grown in either rich or synthetic media lacking leucine. Indeed, total translation of mtDNA was decreased in the EV-transformed strains compared with their untransformed relatives (Supplemental Figure S6A). Further, Cox3p stability notably differed in the untransformed versus the EV-transformed WT strain (Supplemental Figure S6E); Cox3p was notably more stable in the untransformed WT strain. These results indicate that both mtDNA translation and the stability of its newly produced polypeptides are sensitive to either the growth conditions used and/or the presence of an episomal plasmid.

Therefore, we asked whether acute Aac2p inhibition with BKA increases the turnover of nascent Cox3p in untransformed WT and *aac2*^{A137D} yeast (Figure 8). Indeed, BKA treatment enhanced the turnover of Cox3p in the WT strain expressing endogenous Aac2p, although its rate of degradation was not as fast as in *aac2*^{A137D} yeast (Figure 8E). As expected, BKA treatment did not further increase the turnover of Cox3p in *aac2*^{A137D} yeast. The stability of other newly translated proteins was unaffected by acute Aac2p inhibition except for Atp6p, whose turnover was modestly increased in BKA-treated WT yeast (Figure 8, C–H). These results demonstrate that the stability of nascent Cox3p is dependent on Aac2p transport activity.

DISCUSSION

Consistent with its role as the main conduit for ADP and ATP across the inner membrane, yeast lacking Aac2p activity, due to gene deletion or destabilizing mutations (Nelson *et al.*, 1993; Heidkämper *et al.*, 1996; Müller *et al.*, 1996, 1997), are unable to grow on respiratory media due to a complete block in OXPHOS (Lawson *et al.*, 1990). What is perhaps surprising is that the absence of Aac2p

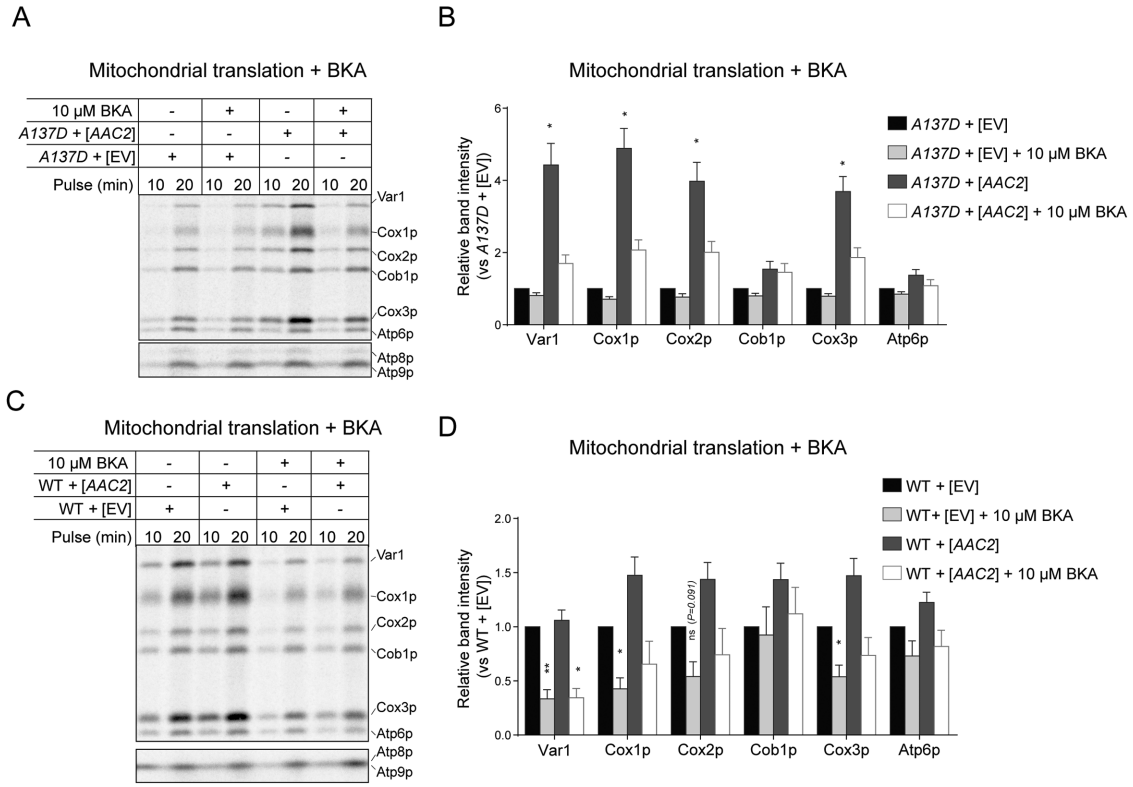

FIGURE 7: Mitochondrial translation is altered by acute Aac2p inhibition. (A) Mitochondrial translation was performed in the absence or presence of 10 μM BKA. Samples were harvested after 10 and 20 min of incubation, resolved by 17.5% SDS–PAGE, and bands identified by phosphoimaging. (B) The relative band intensities for the translated mitochondrial polypeptides in A were quantified and expressed as a ratio compared with the signal detected in the *A137D* strain transformed with empty vector (EV) in the absence of BKA. Mean ± SEM, $n = 4$. Only statistically significant differences relative to *A137D*+ [EV] in absence of BKA are displayed. (C) Mitochondrial translation was performed in the absence or presence of 10 μM BKA. Samples were harvested after 10 and 20 min incubation, resolved by 17.5% SDS–PAGE, and bands identified by phosphoimaging. (D) The relative band intensities for the translated mitochondrial polypeptides in C were quantified and expressed as a ratio compared with the signal detected in the WT strain transformed with empty vector in the absence of BKA. Mean ± SEM, $n = 4$. Only statistically significant differences relative to WT + [EV] in absence of BKA are displayed.

specifically impairs the function of complex IV, but not complex III (Figure 2, A–D; Dienhart and Stuart, 2008). Potential insight into the underlying mechanism, which has remained unresolved for more than 20 yr, was provided by the demonstration that Aac2p physically associates with respiratory supercomplexes consisting of complexes III and IV (Claypool *et al.*, 2008; Dienhart and Stuart, 2008). The goal of the present study was to determine whether complex IV activity is dependent on its physical association with Aac2p or instead Aac2p-mediated ADP/ATP transport. Utilizing a transport-null Aac2p mutant to distinguish between these possibilities, we have established that robust complex IV function requires Aac2p-based transport and not its physical association. In fact, if anything, the transport-null allele, which retained its ability to associate with complex IV–containing supercomplexes, resulted in more severe phenotypes than when Aac2p was completely missing.

How does the absence of Aac2p activity specifically impair complex IV function? Initial insight into the underlying mechanism was that the steady-state amount of all three complex IV subunits encoded by the mitochondrial genome was significantly reduced when Aac2p function is missing. As expected, the levels of mtDNA in strains lacking Aac2p function were normal (Kovác *et al.*, 1967). In yeast, mitochondrial transcription can be regulated by nucleotide levels through the ability of the mitochondrial RNA polymerase, Rpo41p, to sense fluctuations in ATP levels (Amiott and Jaehning, 2006; Asin-Cayuela and Gustafsson, 2007). However, even though the absence of Aac2p activity resulted in altered mitochondrial ADP and ATP levels and a disturbed ADP:ATP ratio, mtDNA transcript levels were not affected, consistent with a prior study (Kucejova *et al.*, 2008). Although the abundance of mtDNA transcripts was normal in the absence of Aac2p function, their subsequent translation was not. Whereas the synthesis of Cox1-3p was reduced, the translation of mtDNA-encoded complex V subunits was increased. Curiously, although the steady-state amount of Cox1-3p mirrored their translation, this was not the case for the complex V subunits. Overall, these findings indicate that although mitochondrial translation is not globally impaired by the absence of Aac2p function, it is significantly dysregulated.

One potential explanation for the reduced translation of COX subunits when Aac2p activity is missing is that the assembly of complex IV, which is known to tightly regulate translation of subunits through feedback mechanisms, is impaired. For example, a 15–base pair deletion in human Cox3p which decreases its stability additionally reduces the synthesis and stability of Cox1p and Cox2p and impairs the assembly of complex IV (Hoffbuhr *et al.*, 2000). In yeast, Cox1p synthesis is significantly decreased by mutations in *COX2* or the *COX3* translational activators, *PET54 and PET122*, in a way that

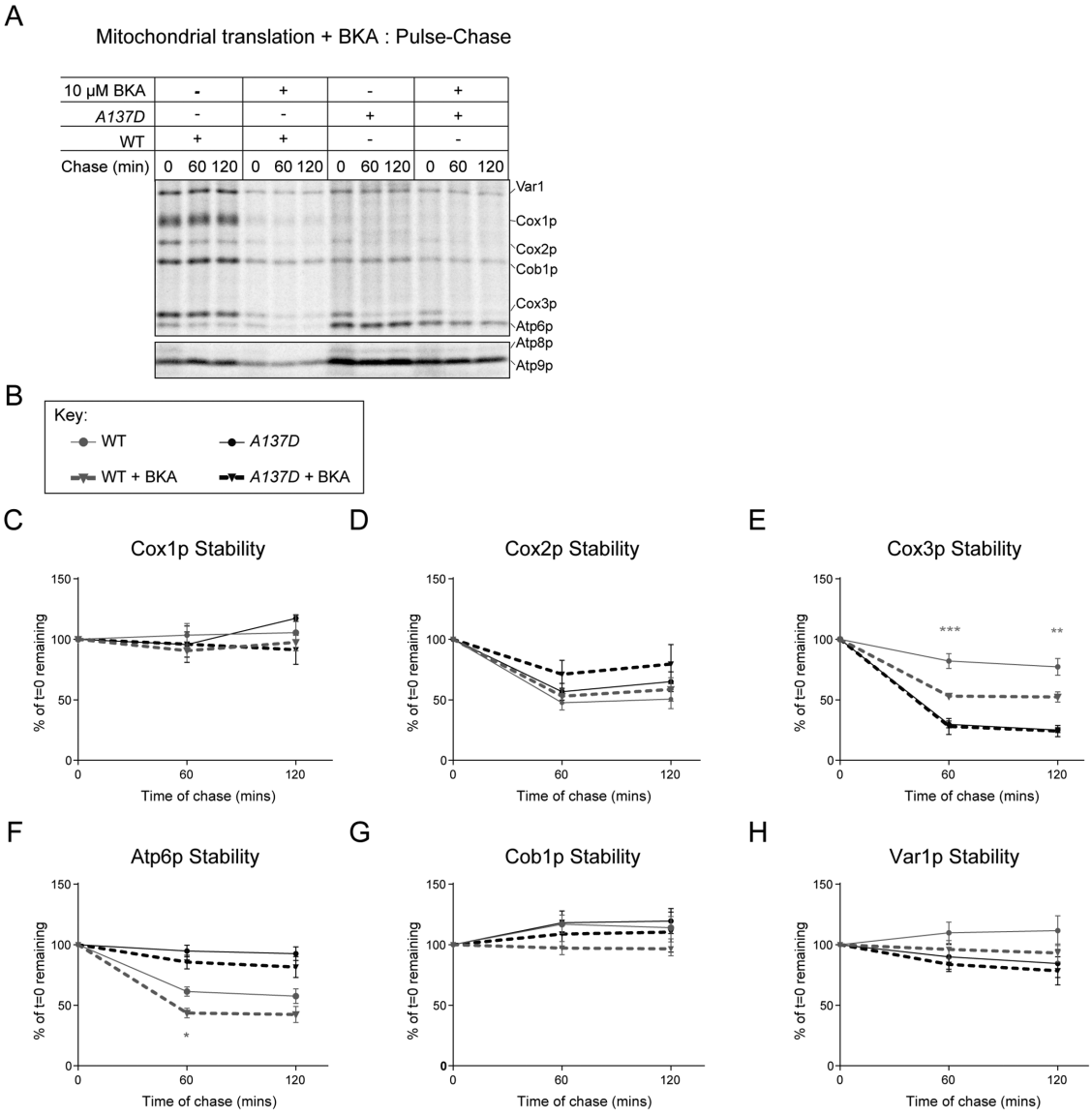

FIGURE 8: The stability of nascent Cox3p is reduced by acute Aac2p inhibition. (A) Mitochondrial translation was performed in the absence or presence of 10 μM BKA. After 20 min of pulse, 4 μg/ml puromycin and 24.2 μM cold Met/Cys were added and samples collected at $t = 0$ and after 60 and 120 min of chase. Extracts were resolved on 17.5% SDS–PAGE, and bands identified by phosphoimaging. (B) Key for quantitations presented in C–H. The relative signal for mitochondrial translated products in the pulse-chase experiment was quantified taking the signal at $t = 0$ as 100%. Mean ± SEM, $n = 4$. Significant differences (as determined by two-way ANOVA with Sidak's multiple comparison test) in BKA-treated vs. untreated samples are shown.

appears to be mediated by the assembly status of complex IV (Shingú-Vázquez *et al.*, 2010). However, not only was complex IV assembly normal at steady state, the kinetics of its assembly was the same in the presence or absence of Aac2p function. An assembly defect could lead to accumulation of unassembled polypeptides and/or assembly intermediates that could become toxic if not resolved. However, deletion of Oma1p, which is involved in the degradation of unassembled subunits of complex IV in certain situations (Bestwick *et al.*, 2010; Khalimonchuk *et al.*, 2012), did not rescue the steady-state level of complex IV subunits when Aac2p function is missing (Supplemental Figure S7). In humans, truncating mutations in *COX1* have been shown to destabilize other complex IV subunits via a mechanism that requires the activity of the *m*-AAA protease even though the truncated Cox1p polypeptide is still able to assemble with other complex IV subunits as well as other respiratory complexes (Hornig-Do *et al.*, 2012). Unfortunately, potential roles for the two mitochondrial AAA proteases Yme1p and Yta10p/Yta12p have not been determined because loss of Aac2p function is synthetically lethal with *yme1Δ* (Wang *et al.*, 2008) and complex IV subunits do not accumulate in the absence of Yta10p/Yta12p (Arlt *et al.*, 1998). These results suggest that the low steady-state amounts of mtDNA-encoded complex IV subunits in the absence of Aac2p activity stems from their reduced translation and not from a complex IV assembly defect.

Interestingly, the complex IV–related perturbations were greater in the context of the transport-null Aac2p mutant than when Aac2p was entirely gone. This was not due to compensation by the minor Aac isoforms because the same trend was observed in the presence

and absence of Aac1p and Aac3p. Interestingly, the stability of newly translated Cox3p was compromised in yeast expressing the inactive Aac2p mutant but not in yeast lacking Aac2p altogether. Similarly, inhibition of Aac2p with BKA also specifically increased the turnover of Cox3p in WT yeast. We speculate that the reduced stability of nascent Cox3p may contribute to the more drastic decrease in steady-state levels of mtDNA-encoded complex IV subunits in *aac2*^{A137D} versus *aac2*Δ mitochondria. These results raise the possibility that a high ATP-demanding process exists that is required for the stability of newly made but unassembled Cox3p. Moreover, the increased turnover of nascent Cox3p only occurs when Aac2p is present but nonfunctional suggesting that Aac2p facilitates the degradation of Cox3p via an activity that is distinct from its role in ADP/ATP exchange. Another potential explanation for the more severe complex IV phenotype of the transport-null Aac2p mutant was based on the identification of Mss51p as a potential Aac2p binding partner (Claypool *et al.*, 2008). If the ability of Mss51p to stimulate *COX1* translation is reduced when bound to Aac2p, then this could in turn help explain the relatively strong *aac2*^{A137D} phenotype. However, because Mss51p overexpression failed to improve *COX1* translation when Aac2p activity was missing, the latter scenario appears unlikely.

The altered pattern of translation we observed is similar to what has been reported for loss-of-function mutants of the mitochondrial translation initiation factor, Aim23p; the DEAD-box helicase and mitochondrial transcription elongation factor, Mss116p; and the protein subunit of mitochondrial RNase P, Rpm2p, which is involved in mitochondrial RNA processing and mitochondrial translation (Stribinskis *et al.*, 2001; Kuzmenko *et al.*, 2016; De Silva *et al.*, 2017). We wondered whether the absence of Aac2p function regulates mitochondrial translation in a way that is dependent on any of these mitochondrial proteins. Focusing on Aim23p, we asked whether overexpression of this protein could rescue the impairment of mitochondrial translation that we observed in the absence of Aac2p function. Overexpression of Aim23p and Mss51p did not rescue the translation impairment, suggesting that the absence of Aac2p function impacts mitochondrial translation in a way that does not involve either of these two proteins. Surprisingly, the restored translation of complex IV subunits provided by overexpressed WT Aac2p was completely prevented by the inclusion of the Aac2p inhibitor, BKA. Because the chronic absence of Aac2p function significantly altered the mitochondrial ADP:ATP ratio (Figure 1I), these results imply that Aac2p-based transport has an active and direct role in mitochondrial translation that may involve a feedback mechanism that is sensitive to matricial nucleotide levels. Even though some of the regulatory mechanisms that control mitochondrial translation are notably different between yeast and metazoans (Kehrein *et al.*, 2013), it will be important to determine whether mitochondrial translation in humans is similarly dependent on mitochondrial ADP/ATP transport. If this requirement is conserved, then this could provide novel insight into ANT-associated diseases (Graham *et al.*, 1997; Kaukonen *et al.*, 2000; Jordens *et al.*, 2002; Komaki *et al.*, 2002; Fontanesi *et al.*, 2004; Palmieri *et al.*, 2005; Sharer, 2005; Echaniz-Laguna *et al.*, 2012; Vandewalle *et al.*, 2013; Thompson *et al.*, 2016).

MATERIALS AND METHODS

Yeast strains and growth conditions

All yeast strains used in this study were derived from GA74-1A (*MAT*a, *his3-11,15*, *leu2*, *ura3*, *trp1*, *ade8* [*rho*$^+$, *mit*$^+$]). *aac1*Δ::*TRP1* and *aac3*Δ::*HISMX6* were established by replacing the entire open reading frame of the gene using PCR-mediated gene replacement (Wach *et al.*, 1994). *aac1*Δ*aac3*Δ (*MAT*a, *trp1*, *leu2*, *ura3*, *ade8*, *aac1*Δ::*TRP1*, *aac3*Δ::*HISMX6*) was generated from *aac1*Δ (*MAT*a, *his3-11,15*, *trp1*, *leu2*, *ura3*, *ade8*, *aac1*Δ::*TRP1*). *aac2*Δ, *aac2*^{A137D}, and *aac1*Δ*aac3*Δ*aac2*Δ*aac1*Δ*aac3*Δ*aac2*^{A137D} were generated from WT and *aac1*Δ*aac3*Δ strains using a homology-integrated CRISPR-Cas (HI-CRISPR) system as previously described but with slight modification (Bao *et al.*, 2015; Ogunbona *et al.*, 2017). Briefly, the CRISPR-Cas9 target for *AAC2* was selected using the Web-based yeastriction (Mans *et al.*, 2015) and Benchling CRISPR guide design tools. The CRISPR construct was designed to recognize residues 542–561 on the reverse strand of *AAC2* (position 1 is the adenine of the AUG site). A 99–base pair or 250–base pair homology repair template was designed to have homology arms on both sides flanking the Cas9 cutting site and incorporated an 8–base pair deletion or point mutations to generate *aac2*Δ and *aac2*^{A137D}, respectively. *oma1*Δ strains were generated from the corresponding parental strains as previously described (Ogunbona *et al.*, 2017).

Cox8p and Qcr10p, subunits of complex IV and complex III, respectively, were endogenously tagged in WT, *aac2*Δ, and *aac2*^{A137D} strains on the C-terminal end with 3X FLAG epitope tag using PCR-mediated gene replacement (Wach *et al.*, 1994). *COX5A* and *COX13* genomic sequences were amplified from GA74-1A yeast genomic DNA and cloned into pSP64. Aac2p, Mss51^{F199I}p, and Aim23p were overexpressed under the control of their native promoters in WT, *aac2*Δ, and *aac2*^{A137D} strains. *AAC2* and *AIM23* were amplified from genomic DNA isolated from GA74-1A yeast using primers that hybridized approximately 380 base pairs upstream of the predicted start codon and 140 base pairs downstream from the predicted stop codon and cloned into pRS315 and pRS425, respectively. The constitutively active mutant form of *MSS51* (*MSS51*^{F199I}; Barrientos *et al.*, 2002; Fontanesi *et al.*, 2011; De Silva *et al.*, 2017) was subcloned into pRS425.

Yeast cells were grown in either YP-sucrose (1% yeast extract, 2% peptone, 2% sucrose), YP-dextrose (1% yeast extract, 2% peptone, 2% dextrose), or their synthetic (SC) media equivalent (containing 0.17% yeast nitrogen base minus amino acids, 0.5% ammonium sulfate, 0.2% dropout mix containing required amino acids, and 2% sucrose or dextrose). To assess the respiratory function of the different strains, overnight cultures grown in indicated media were spotted on solid media containing 2% dextrose or ethanol/glycerol (1% ethanol, 3% glycerol) and grown at 30°C.

Measurement of ascorbate-TMPD respiration rates

Oxygen consumption rates were measured using a Clark-type oxygen electrode as described before (Claypool *et al.*, 2008), with some modifications. In brief, mitochondria (100 µg) were used as soon as possible after thawing on ice. Respiration buffer (1 ml; 0.25 M sucrose, 0.25 mg/ml bovine serum albumin [BSA], 20 mM KCl, 20 mM Tris-Cl, 0.5 mM EDTA, 4 mM KH_2PO_4, and 3 mM $MgCl_2$, pH 7.2) was added to a magnetically stirred 1.5 ml chamber with temperature controlled at 25°C and the signal representing the level of oxygen in the chamber allowed to equilibrate. Following the addition of mitochondria, background respiration rate was recorded for ~30 s. Next, 1 mM ascorbate and 0.3 mM TMPD were added simultaneously and the state 2 respiration recorded for 1 min, before the addition of 50 µM ADP to initiate state 3 respiration. Once the added ADP was consumed, state 4 respiration was recorded for 2 min before 10 µM carbonyl cyanide-4-(trifluoromethoxy)phenylhydrazone (FCCP) was added to induce uncoupling. Uncoupled respiration was measured for 2 min or until the oxygen level reached zero. As there is no ADP-stimulated respiration in the absence of Aac2p function, the basal respiration (state 2) and uncoupled respiration were calculated.

Spectrophotometric activity assay

Respiratory complex III and IV activities were measured as previously described (Tzagoloff *et al.*, 1975; Dienhart and Stuart, 2008; Lu *et al.*, 2017). Briefly, 5 µg of mitochondria solubilized in 0.5% (wt/vol) *n*-dodecyl β-D-maltoside (Anatrace) and spiked with protease inhibitors was added to reaction buffer (50 mM KPi, 2 mM EDTA, pH 7.4) with 0.08% (wt/vol) equine heart cytochrome *c* (Sigma). For complex III activity measurements, 1 mM KCN (prevents oxidation of cytochrome *c* by complex IV) and 100 µM decylubiquinol (an analogue of coenzyme Q) were added before the reaction was initiated. The reduction or oxidation of cytochrome *c* was followed at 550 nm.

Mitochondrial ADP and ATP measurement

Mitochondrial nucleotide levels were measured using an ApoSENSOR ADP/ATP bioluminescent assay kit (BioVision) according to the manufacturer's protocol. Briefly, luminescence of each crude mitochondrial sample was measured using a BMG Labtech Fluostar Omega microplate reader in the luminescence mode. Mitochondria (50 µg) were added to a mixture of ATP monitoring enzyme and nucleotide releasing buffer incubated at room temperature in a Greiner Bio-One Black flat-bottomed 96-well plate. To determine the ATP level, luminescence values after 2 min of adding mitochondrial samples were corrected by subtracting background luminescence. Thereafter, an ADP-converting enzyme that converts ADP to ATP was added and the ADP levels were determined as the change in luminescence after the converting enzyme was added.

DNA extraction and quantitative real-time PCR

DNA was extracted as described (Hoffman, 2001). In brief, 15 U of A_{600} yeast cells grown for 24–48 h in YP-sucrose media were harvested, washed in sterile water, and resuspended in 200 µl of breaking buffer (2% Triton X-100 [wt/vol], 1% SDS [wt/vol], 100 mM NaCl, 10 mM Tris, pH 8.0, 1 mM EDTA, pH 8.0). Glass beads (0.3 g; ~200–300 µl volume) and 200 µl phenol/chloroform/isoamyl alcohol was added and the tubes sealed with parafilm before vortexing at highest speed for 3 min. Next, 200 µl Tris-EDTA (TE) buffer, pH 8.0, was added and the mixture vortexed briefly before centrifugation at maximum speed at room temperature for 5 min. The aqueous phase was then transferred to a new Eppendorf tube, 1 ml of 100% ethanol added, and then mixed by inversion. This was followed by centrifugation at 21,000 × *g* at room temperature for 3 min and the pellets were resuspended in 400 µl TE buffer, pH 8.0. RNase A (3 µl of 10 mg/ml) was added followed by incubation at 37°C for 5 min before adding 10 µl of 4 M ammonium acetate and 1 ml 100% ethanol. Finally, DNA pellets were recovered by centrifugation at maximum speed at room temperature for 3 min, dried, and then resuspended in 30 µl TE buffer, pH 8.0. The DNA was quantitated and stored at −80°C. Before the analyses, the DNA was requantitated and used at 10 ng/µl as template in the qPCR.

The FastStart Universal SYBR Green Master Rox (Roche) was used for qPCR performed according to the manufacturer's instructions. Genomic DNA (50 ng) was used as template and the following primers were used at 100 nM concentration in a 20 µl reaction: *COX1* forward, 5′-CTACAGATACAGCATTTCCAAGA-3′; *COX1* reverse, 5′-GTGCCTGAATAGATGATAATGGT-3′; *ACT1* forward, 5′-GTATGTGTAAAGCCGGTTTTG-3′; *ACT1* reverse, 5′-CATGATACCTTGGTGTCTTGG-3′. The reaction was done in technical duplicate with three biological replicates. No-template controls were included in every assay. After completion of thermocycling cycles in a QuantStudio 6 Flex Real-Time PCR System (Thermo Fisher), melting-curve data were collected to verify PCR specificity and the absence of primer dimers. The Ct value differences between the nuclear (*ACT1*) and mitochondrial (*COX1*) target were computed as a measure of the level of mtDNA copy number relative to nuclear genome. A strain lacking its mitochondrial genome (Rho null) was used as negative control in all experiments.

RNA extraction and reverse transcription-quantitative real-time PCR

Total RNA was extracted using hot phenol extraction exactly as described (Amin-ul Mannan *et al.*, 2009) except that yeast cells were grown in YP-sucrose media. Following treatment with Turbo DNase to remove any contaminating genomic DNA (TURBO DNA-free Kit; Invitrogen), RNA was purified using a RNeasy MiniElute Cleanup Kit (Qiagen). RNA (1 µg) was reverse-transcribed into cDNA using SuperScript VILO Master Mix (Invitrogen) according to the manufacturer's protocol. The qPCR was done as described above but using a 1:10 dilution of synthesized cDNA as template instead of genomic DNA. Additionally, we performed a minus-RT control, that is, RNA not reverse-transcribed to cDNA to verify the absence of contaminating genomic DNA in RNA samples, in addition to a no-template control. *TAF10* was used as a reference gene (Teste *et al.*, 2009). The primers used are *TAF10* forward, 5′-ATATTCCAGGATCAGGTCTTCCGTAGC-3′; *TAF10* reverse, 5′-GTAGTCTTCTCATTCTGTTGATGTTGTTGTTG-3′; *COX1* forward, 5′-TGCCTGCTTTAATTGGAGGT-3′; *COX1* reverse, 5′-GGTCCTGAATGTGCCTGAAT-3′; *COX2* forward, 5′-TTCAGGATTCAGCAACACCA-3′; *COX2* reverse, 5′-CAGCTGGAAAAATTGTTCAAATA-3′; *COX3* forward, 5′-TCTTTGCTGGTTTATTCTGAGC-3′; *COX3* reverse, 5′-CTGCGATTAAGGCATGATGA-3′; *ATP6* forward, 5′-CCTGCTGGTACACCATTACC-3′; *ATP6* reverse, 5′-AGCCCAGACATATCCCTGAA-3′; *ATP9* forward, 5′-TTGGAGCAGGTATCTCAACAAT-3′; *ATP9* reverse, 5′-GCTTCTGATAAGGCGAAACC-3′. The Ct value differences between the reference gene (nuclear-encoded *TAF10*) and the mitochondrial targets were computed as a measure of the steady-state mRNA levels in the strains. A strain lacking its mitochondrial genome (Rho null) was used as negative control in all experiments.

In vivo labeling of mitochondrial translation products

Yeast cells precultured overnight in either YP-sucrose (1% yeast extract, 2% peptone, 2% sucrose) or when strains are maintaining plasmids, synthetic media (containing 0.17% yeast nitrogen base minus amino acids, 0.5% ammonium sulfate, 0.2% dropout mix containing amino acids except leucine, and 2% sucrose) were reinoculated and grown to an A_{600} of 0.4–1. Yeast cells were labeled, prepared, and resolved by SDS–PAGE as done before (Barrientos *et al.*, 2002) with little modification. In brief, 3.2 U of A_{600} yeast cells were washed with 2 ml of metabolic labeling buffer (40 mM KPi, pH 6.0, 2% sucrose, 2 g/l SC-methionine) once and then incubated in the buffer for 5 min to allow completion of in-progress translation. For BKA inhibition, the pH of the labeling buffer was adjusted to 5.0 with diluted HCl and BKA was added at 10 µM concentration. Freshly prepared cycloheximide (0.2 mg/ml) was then added to stop cytoplasmic translation, followed by the addition of 62 µCi/ml Trans ^{35}S-label (sku 015100907; MP Biomedical; 85% methionine and 15% cysteine). Labeling was performed at 30°C in a water bath for up to 20 min. A mixture of nonradioactive 24.2 µM methionine and cysteine (with 4 µg/ml puromycin in the chase) was added to stop the radiolabeling. After different time points, 0.5 ml aliquots were collected, processed in freshly prepared diluted Rodel buffer (0.24 M NaOH, 0.14 M 2-mercaptoethanol, 1.3 mM phenylmethylsulfonyl fluoride [PMSF]) on ice, and then tricarboxylic acid–precipitated.

Recovered pellets were washed first with 500 mM Tris base and then with distilled water. The final pellet samples were resuspended in a 1:1 mixture of 0.1 M NaOH:2× reducing sample buffer and resolved on custom-made 17.5% SDS–PAGE (Barrientos *et al.*, 2002) and/or 12–16% SDS–PAGE gels (the former as first described [Barrientos *et al.*, 2002] gave better separation of all the mitochondrial proteins except Atp8p and Atp9p; however, using 2× more of ammonium persulfate and *N*,*N*,*N*′,*N*′-tetramethylethane-1,2-diamine, that is, 0.098% wt/vol and 0.071% vol/vol, respectively, gave a 17.5% SDS–PAGE that provided for resolution of all the mitochondrial proteins as seen in Figures 7, C and E, and 8A and Supplemental Figures S5A and S6A). Gels were stained with commassie, destained, dried, and separated radiolabeled proteins visualized by autoradiography.

In organello import

This was done as described before (Brandner *et al.*, 2005; Ogunbona *et al.*, 2017) with little modification. In brief, radiolabeled Cox5Ap and Cox13p precursors were synthesized in a coupled transcription/translation reaction (Promega TNT Kit Mix) using 104 µCi of Easy-Tag L-[^{35}S]-Methionine (PerkinElmer Life Sciences) and 5.2 µg of plasmid in a 260 µl reaction volume. Mitochondria (180 µg) were added to import buffer (0.6 M sorbitol, 2 mM KH_2PO_4, 60 mM KCl, 50 mM HEPES, 10 mM $MgCl_2$, 2.5 mM EDTA, pH 8.0, 5 mM L-methionine, 10 mg/ml fatty acid free BSA) containing 2 mM ATP, 2 mM NADH, and an energy-regenerating system (0.1 mg/ml creatine phosphokinase, 1 mM creatine phosphate, 10 mM succinate). Where indicated, the mitochondrial membrane potential was collapsed with 1 µM valinomycin and 5 µM carbonyl cyanide *m*-chlorophenyl hydrazine. Following addition of the radiolabeled precursor, import reactions were incubated at 30°C. At the designated timepoints, import was stopped with an equal volume of ice-cold BB7.4 (0.6 M sorbitol and 20 mM HEPES-KOH, pH 7.4) that contained 40 µg/ml trypsin to degrade nonimported precursors. After at least 30 min on ice, 100 µg/ml soybean trypsin inhibitor was added to each reaction which was then split into two equal portions. To monitor import, mitochondria were recovered by spinning at 21,000 × *g* for 5 min at 4°C and resolved on 15% SDS–PAGE gels. To monitor assembly, the reisolated mitochondria were solubilized in lysis buffer (1% [wt/vol] digitonin, 20 mM HEPE-KOH, pH 7.4, 100 mM NaCl, 20 mM imidazole, 1 mM $CaCl_2$, 10% glycerol, 1 mM PMSF, 10 µM leupeptin, 2 µM pepstatin A) and resolved on 5–12% BN–PAGE gels. Relative to each timempoint, 5% of imported precursors were resolved on 15% SDS–PAGE gels. Radioactive bands were visualized by phosphorimaging.

Antibodies

Most antibodies used in this study were generated in our laboratory or in the laboratories of J. Schatz (University of Basel, Basel, Switzerland) or C. Koehler (University of California, Los Angeles [UCLA]) and have been described previously (Hwang *et al.*, 2007; Claypool *et al.*, 2011; Whited *et al.*, 2013; Onguka *et al.*, 2015; Ogunbona *et al.*, 2017). Other antibodies used were rabbit polyclonal against Atp4p (Dienhart and Stuart, 2008), Atp6p/Atp9p (Kabala *et al.*, 2014), Mss51p (Barrientos *et al.*, 2002), Cox5Ap (Liu and Barrientos, 2013), Qcr7p (Hildenbeutel *et al.*, 2014), and Aim23p (Kuzmenko *et al.*, 2016).

Miscellaneous

Isolation of mitochondria, one-dimensional (1D) BN–PAGE, coimmunoprecipitation, and immunoblotting were performed as previously described (Claypool *et al.*, 2002, 2006, 2011; Onguka *et al.*, 2015; Ogunbona *et al.*, 2017). Band densitometry analyses were performed using Quantity One (Bio-Rad). Statistical comparisons were performed by using one- or two-way analysis of variance (ANOVA) with Dunnett test correction (Sidak's test correction for data shown in Figure 8, C–H, and Supplemental Figure S5, C–H) for multiple comparison in Prism 7 (GraphPad); $P \leq 0.05$ were deemed significant (ns, $P > 0.05$; *, $P \leq 0.05$; **, $P \leq 0.01$; ***, $P \leq 0.001$; ****, $P \leq 0.0001$). All graphs show the mean ± SEM.

ACKNOWLEDGMENTS

We thank Carla Koehler (UCLA), Antoni Barrientos (University of Miami), Jean-Paul Lasserre (University of Bordeaux), Alexander Tzagoloff (Columbia University), Martin Ott (Stockholm University), and Rosemary Stuart (Marquette University) for generous gifts of antibodies and Flavia Fontanesi (University of Miami) for the gift of the Mss51 plasmid. This work was supported by the National Institutes of Health under Grant no. R01HL108882 to S.M.C. and Biochemistry, Cellular, and Molecular Biology Program T32 Training Grant no.T32GM007445 to M.G.B. and by American Heart Association predoctoral fellowships 15PRE24480066 to O.B.O. and 10PRE3280013 to M.G.B.

REFERENCES

Acín-Pérez R, Fernández-Silva P, Peleato ML, Pérez-Martos A, Enriquez JA (2008). Respiratory active mitochondrial supercomplexes. Mol Cell 32, 529–539.

Amin-ul Mannan M, Sharma S, Ganesan K (2009). Total RNA isolation from recalcitrant yeast cells. Anal Biochem 389, 77–79.

Amiott EA, Jaehning JA (2006). Mitochondrial transcription is regulated via an ATP "sensing" mechanism that couples RNA abundance to respiration. Mol Cell 22, 329–338.

Arlt H, Steglich G, Perryman R, Guiard B, Neupert W, Langer T (1998). The formation of respiratory chain complexes in mitochondria is under the proteolytic control of the m-AAA protease. EMBO J 17, 4837–4847.

Asin-Cayuela J, Gustafsson CM (2007). Mitochondrial transcription and its regulation in mammalian cells. Trends Biochem Sci 32, 111–117.

Atkinson GC, Kuzmenko A, Kamenski P, Vysokikh MY, Lakunina V, Tankov S, Smirnova E, Soosaar A, Tenson T, Hauryliuk V (2012). Evolutionary and genetic analyses of mitochondrial translation initiation factors identify the missing mitochondrial IF3 in *S. cerevisiae*. Nucleic Acids Res 40, 6122–6134.

Bao Z, Xiao H, Liang J, Zhang L, Xiong X, Sun N, Si T, Zhao H (2015). Homology-integrated CRISPR-Cas (HI-CRISPR) system for one-step multigene disruption in *Saccharomyces cerevisiae*. ACS Synth Biol 4, 585–594.

Barrientos A, Korr D, Tzagoloff A (2002). Shy1p is necessary for full expression of mitochondrial COX1 in the yeast model of Leigh's syndrome. EMBO J 21, 43–52.

Barrientos A, Zambrano A, Tzagoloff A (2004). Mss51p and Cox14p jointly regulate mitochondrial Cox1p expression in *Saccharomyces cerevisiae*. EMBO J 23, 3472–3482.

Bestwick M, Khalimonchuk O, Pierrel F, Winge DR (2010). The role of Coa2 in hemylation of yeast Cox1 revealed by its genetic interaction with Cox10. Mol Cell Biol 30, 172–185.

Brandner K, Mick DU, Frazier AE, Taylor RD, Meisinger C, Rehling P (2005). Taz1, an outer mitochondrial membrane protein, affects stability and assembly of inner membrane protein complexes: implications for Barth syndrome. Mol Biol Cell 16, 5202–5214.

Claypool SM, Dickinson BL, Yoshida M, Lencer WI, Blumberg RS (2002). Functional reconstitution of human FcRn in Madin-Darby canine kidney cells requires co-expressed human β_2-microglobulin. J Biol Chem 277, 28038–28050.

Claypool SM, McCaffery JM, Koehler CM (2006). Mitochondrial mislocalization and altered assembly of a cluster of Barth syndrome mutant tafazzins. J Cell Biol 174, 379–390.

Claypool SM, Oktay Y, Boontheung P, Loo JA, Koehler CM (2008). Cardiolipin defines the interactome of the major ADP/ATP carrier protein of the mitochondrial inner membrane. J Cell Biol 182, 937–950.

Claypool SM, Whited K, Srijumnong S, Han X, Koehler CM (2011). Barth syndrome mutations that cause tafazzin complex lability. J Cell Biol 192, 447–462.

De Silva D, Poliquin S, Zeng R, Zamudio-Ochoa A, Marrero N, Perez-Martinez X, Fontanesi F, Barrientos A (2017). The DEAD-box helicase Mss116 plays distinct roles in mitochondrial ribogenesis and mRNA-specific translation. Nucleic Acids Res 45, 6628–6643.
Dienhart MK, Stuart RA (2008). The yeast Aac2 protein exists in physical association with the cytochrome bc1-COX supercomplex and the TIM23 machinery. Mol Biol Cell 19, 3934–3943.
Doerner A, Pauschinger M, Badorff A, Noutsias M, Giessen S, Schulze K, Bilger J, Rauch U, Schultheiss HP (1997). Tissue-specific transcription pattern of the adenine nucleotide translocase isoforms in humans. FEBS Lett 414, 258–262.
Dolce V, Scarcia P, Iacopetta D, Palmieri F (2005). A fourth ADP/ATP carrier isoform in man: identification, bacterial expression, functional characterization and tissue distribution. FEBS Lett 579, 633–637.
Dupont PY, Stepien G (2011). Computational analysis of the transcriptional regulation of the adenine nucleotide translocator isoform 4 gene and its role in spermatozoid glycolytic metabolism. Gene 487, 38–45.
Echaniz-Laguna A, Chassagne M, Ceresuela J, Rouvet I, Padet S, Acquaviva C, Nataf S, Vinzio S, Bozon D, Mousson de Camaret B (2012). Complete loss of expression of the ANT1 gene causing cardiomyopathy and myopathy. J Med Genet 49, 146–150.
Fontanesi F, Clemente P, Barrientos A (2011). Cox25 teams up with Mss51, Ssc1, and Cox14 to regulate mitochondrial cytochrome *c* oxidase subunit 1 expression and assembly in *Saccharomyces cerevisiae*. J Biol Chem 286, 555–566.
Fontanesi F, Palmieri L, Scarcia P, Lodi T, Donnini C, Limongelli A, Tiranti V, Zeviani M, Ferrero I, Viola AM (2004). Mutations in AAC2, equivalent to human adPEO-associated ANT1 mutations, lead to defective oxidative phosphorylation in *Saccharomyces cerevisiae* and affect mitochondrial DNA stability. Hum Mol Genet 13, 923–934.
Gavurníková G, Sabova L, Kissová I, Haviernik P, Kolarov J (1996). Transcription of the AAC1 gene encoding an isoform of mitochondrial ADP/ATP carrier in *Saccharomyces cerevisiae* is regulated by oxygen in a heme-independent manner. Eur J Biochem 239, 759–763.
Graham BH, Waymire KG, Cottrell B, Trounce IA, MacGregor GR, Wallace DC (1997). A mouse model for mitochondrial myopathy and cardiomyopathy resulting from a deficiency in the heart/muscle isoform of the adenine nucleotide translocator. Nat Genet 16, 226–234.
Gu J, Wu M, Guo R, Yan K, Lei J, Gao N, Yang M (2016). The architecture of the mammalian respirasome. Nature 537, 639–643.
Heidkämper D, Müller V, Nelson DR, Klingenberg M (1996). Probing the role of positive residues in the ADP/ATP carrier from yeast. The effect of six arginine mutations on transport and the four ATP versus ADP exchange modes. Biochemistry 35, 16144–16152.
Hildenbeutel M, Hegg EL, Stephan K, Gruschke S, Meunier B, Ott M (2014). Assembly factors monitor sequential hemylation of cytochrome b to regulate mitochondrial translation. J Cell Biol 205, 511–524.
Hoffbuhr KC, Davidson E, Filiano BA, Davidson M, Kennaway NG, King MP (2000). A pathogenic 15-base pair deletion in mitochondrial DNA-encoded cytochrome *c* oxidase subunit III results in the absence of functional cytochrome *c* oxidase. J Biol Chem 275, 13994–14003.
Hoffman CS (2001). Preparation of yeast DNA. Curr Protoc Mol Biol Chapter 13, Unit 13.11.
Hornig-Do HT, Tatsuta T, Buckermann A, Bust M, Kollberg G, Rötig A, Hellmich M, Nijtmans L, Wiesner RJ (2012). Nonsense mutations in the COX1 subunit impair the stability of respiratory chain complexes rather than their assembly. EMBO J 31, 1293–1307.
Hwang DK, Claypool SM, Leuenberger D, Tienson HL, Koehler CM (2007). Tim54p connects inner membrane assembly and proteolytic pathways in the mitochondrion. J Cell Biol 178, 1161–1175.
Jordens EZ, Palmieri L, Huizing M, van den Heuvel LP, Sengers RC, Dörner A, Ruitenbeek W, Trijbels FJ, Valsson J, Sigfusson G, *et al*. (2002). Adenine nucleotide translocator 1 deficiency associated with Sengers syndrome. Ann Neurol 52, 95–99.
Kabala AM, Lasserre JP, Ackerman SH, di Rago JP, Kucharczyk R (2014). Defining the impact on yeast ATP synthase of two pathogenic human mitochondrial DNA mutations, T9185C and T9191C. Biochimie 100, 200–206.
Kaukonen J, Juselius JK, Tiranti V, Kyttälä A, Zeviani M, Comi GP, Keränen S, Peltonen L, Suomalainen A (2000). Role of adenine nucleotide translocator 1 in mtDNA maintenance. Science 289, 782–785.
Kehrein K, Bonnefoy N, Ott M (2013). Mitochondrial protein synthesis: efficiency and accuracy. Antioxid Redox Signal 19, 1928–1939.
Khalimonchuk O, Jeong MY, Watts T, Ferris E, Winge DR (2012). Selective Oma1 protease-mediated proteolysis of Cox1 subunit of cytochrome oxidase in assembly mutants. J Biol Chem 287, 7289–7300.
Klingenberg M (2008). The ADP and ATP transport in mitochondria and its carrier. Biochim Biophys Acta 1778, 1978–2021.
Kokoszka JE, Waymire KG, Flierl A, Sweeney KM, Angelin A, MacGregor GR, Wallace DC (2016). Deficiency in the mouse mitochondrial adenine nucleotide translocator isoform 2 gene is associated with cardiac noncompaction. Biochim Biophys Acta 1857, 1203–1212.
Komaki H, Fukazawa T, Houzen H, Yoshida K, Nonaka I, Goto Y (2002). A novel D104G mutation in the adenine nucleotide translocator 1 gene in autosomal dominant progressive external ophthalmoplegia patients with mitochondrial DNA with multiple deletions. Ann Neurol 51, 645–648.
Kovác L, Lachowicz TM, Slonimski PP (1967). Biochemical genetics of oxidative phosphorylation. Science 158, 1564–1567.
Kucejova B, Li L, Wang X, Giannattasio S, Chen XJ (2008). Pleiotropic effects of the yeast Sal1 and Aac2 carriers on mitochondrial function via an activity distinct from adenine nucleotide transport. Mol Genet Genomics 280, 25–39.
Kuzmenko A, Atkinson GC, Levitskii S, Zenkin N, Tenson T, Hauryliuk V, Kamenski P (2014). Mitochondrial translation initiation machinery: conservation and diversification. Biochimie 100, 132–140.
Kuzmenko A, Derbikova K, Salvatori R, Tankov S, Atkinson GC, Tenson T, Ott M, Kamenski P, Hauryliuk V (2016). Aim-less translation: loss of *Saccharomyces cerevisiae* mitochondrial translation initiation factor mIF3/Aim23 leads to unbalanced protein synthesis. Sci Rep 6, 18749.
Lawson JE, Gawaz M, Klingenberg M, Douglas MG (1990). Structure-function studies of adenine nucleotide transport in mitochondria. I. Construction and genetic analysis of yeast mutants encoding the ADP/ATP carrier protein of mitochondria. J Biol Chem 265, 14195–14201.
Letts JA, Fiedorczuk K, Sazanov LA (2016). The architecture of respiratory supercomplexes. Nature 537, 644–648.
Liu J, Barrientos A (2013). Transcriptional regulation of yeast oxidative phosphorylation hypoxic genes by oxidative stress. Antioxid Redox Signal 19, 1916–1927.
Lu YW, Acoba MG, Selvaraju K, Huang TC, Nirujogi RS, Sathe G, Pandey A, Claypool SM (2017). Human adenine nucleotide translocases physically and functionally interact with respirasomes. Mol Biol Cell 28, 1489–1506.
Maldonado EN, DeHart DN, Patnaik J, Klatt SC, Gooz MB, Lemasters JJ (2016). ATP/ADP turnover and import of glycolytic ATP into mitochondria in cancer cells is independent of the adenine nucleotide translocator. J Biol Chem 291, 19642–19650.
Mans R, van Rossum HM, Wijsman M, Backx A, Kuijpers NG, van den Broek M, Daran-Lapujade P, Pronk JT, van Maris AJ, Daran JM (2015). CRISPR/Cas9: a molecular Swiss army knife for simultaneous introduction of multiple genetic modifications in *Saccharomyces cerevisiae*. FEMS Yeast Res 15, fov004.
McStay GP, Su CH, Thomas SM, Xu JT, Tzagoloff A (2013a). Characterization of assembly intermediates containing subunit 1 of yeast cytochrome oxidase. J Biol Chem 288, 26546–26556.
McStay GP, Su CH, Tzagoloff A (2013b). Modular assembly of yeast cytochrome oxidase. Mol Biol Cell 24, 440–452.
Mick DU, Vukotic M, Piechura H, Meyer HE, Warscheid B, Deckers M, Rehling P (2010). Coa3 and Cox14 are essential for negative feedback regulation of COX1 translation in mitochondria. J Cell Biol 191, 141–154.
Moreno-Lastres D, Fontanesi F, García-Consuegra I, Martín MA, Arenas J, Barrientos A, Ugalde C (2012). Mitochondrial complex I plays an essential role in human respirasome assembly. Cell Metab 15, 324–335.
Müller V, Basset G, Nelson DR, Klingenberg M (1996). Probing the role of positive residues in the ADP/ATP carrier from yeast. The effect of six arginine mutations of oxidative phosphorylation and AAC expression. Biochemistry 35, 16132–16143.
Müller V, Heidkämper D, Nelson DR, Klingenberg M (1997). Mutagenesis of some positive and negative residues occurring in repeat triad residues in the ADP/ATP carrier from yeast. Biochemistry 36, 16008–16018.
Nelson DR, Lawson JE, Klingenberg M, Douglas MG (1993). Site-directed mutagenesis of the yeast mitochondrial ADP/ATP translocator. Six arginines and one lysine are essential. J Mol Biol 230, 1159–1170.
Ogunbona OB, Onguka O, Calzada E, Claypool SM (2017). Multitiered and cooperative surveillance of mitochondrial Phosphatidylserine Decarboxylase 1. Mol Cell Biol 37, e00049-17.
Onguka O, Calzada E, Ogunbona OB, Claypool SM (2015). Phosphatidylserine decarboxylase 1 autocatalysis and function does not require a mitochondrial-specific factor. J Biol Chem 290, 12744–12752.
Palmieri L, Alberio S, Pisano I, Lodi T, Meznaric-Petrusa M, Zidar J, Santoro A, Scarcia P, Fontanesi F, Lamantea E, *et al*. (2005). Complete loss-of-function of the heart/muscle-specific adenine nucleotide translocator is

associated with mitochondrial myopathy and cardiomyopathy. Hum Mol Genet 14, 3079–3088.
Perez-Martinez X, Broadley SA, Fox TD (2003). Mss51p promotes mitochondrial Cox1p synthesis and interacts with newly synthesized Cox1p. EMBO J 22, 5951–5961.
Perez-Martinez X, Butler CA, Shingu-Vazquez M, Fox TD (2009). Dual functions of Mss51 couple synthesis of Cox1 to assembly of cytochrome *c* oxidase in *Saccharomyces cerevisiae* mitochondria. Mol Biol Cell 20, 4371–4380.
Sabová L, Zeman I, Supek F, Kolarov J (1993). Transcriptional control of AAC3 gene encoding mitochondrial ADP/ATP translocator in *Saccharomyces cerevisiae* by oxygen, heme and ROX1 factor. Eur J Biochem 213, 547–553.
Schägger H (2001). Respiratory chain supercomplexes. IUBMB Life 52, 119–128.
Schägger H, Pfeiffer K (2000). Supercomplexes in the respiratory chains of yeast and mammalian mitochondria. EMBO J 19, 1777–1783.
Sharer JD (2005). The adenine nucleotide translocase type 1 (ANT1): a new factor in mitochondrial disease. IUBMB Life 57, 607–614.
Shingú-Vázquez M, Camacho-Villasana Y, Sandoval-Romero L, Butler CA, Fox TD, Pérez-Martínez X (2010). The carboxyl-terminal end of Cox1 is required for feedback assembly regulation of Cox1 synthesis in *Saccharomyces cerevisiae* mitochondria. J Biol Chem 285, 34382–34389.
Siep M, van Oosterum K, Neufeglise H, van der Spek H, Grivell LA (2000). Mss51p, a putative translational activator of cytochrome *c* oxidase subunit-1 (COX1) mRNA, is required for synthesis of Cox1p in *Saccharomyces cerevisiae*. Curr Genet 37, 213–220.
Soto IC, Fontanesi F, Liu J, Barrientos A (2012). Biogenesis and assembly of eukaryotic cytochrome *c* oxidase catalytic core. Biochim Biophys Acta 1817, 883–897.
Stepien G, Torroni A, Chung AB, Hodge JA, Wallace DC (1992). Differential expression of adenine nucleotide translocator isoforms in mammalian tissues and during muscle cell differentiation. J Biol Chem 267, 14592–14597.
Stribinskis V, Gao GJ, Ellis SR, Martin NC (2001). Rpm2, the protein subunit of mitochondrial RNase P in *Saccharomyces cerevisiae*, also has a role in the translation of mitochondrially encoded subunits of cytochrome *c* oxidase. Genetics 158, 573–585.
Su CH, McStay GP, Tzagoloff A (2014). The Cox3p assembly module of yeast cytochrome oxidase. Mol Biol Cell 25, 965–976.
Teste MA, Duquenne M, François JM, Parrou JL (2009). Validation of reference genes for quantitative expression analysis by real-time RT-PCR in *Saccharomyces cerevi*siae. BMC Mol Biol 10, 99.
Thompson K, Majd H, Dallabona C, Reinson K, King MS, Alston CL, He L, Lodi T, Jones SA, Fattal-Valevski A, *et al*. (2016). Recurrent de novo dominant mutations in SLC25A4 cause severe early-onset mitochondrial disease and loss of mitochondrial DNA copy number. Am J Hum Genet 99, 1405.
Towpik J (2005). Regulation of mitochondrial translation in yeast. Cell Mol Biol Lett 10, 571–594.
Tzagoloff A, Akai A, Needleman RB (1975). Assembly of the mitochondrial membrane system: isolation of nuclear and cytoplasmic mutants of *Saccharomyces cerevisiae* with specific defects in mitochondrial functions. J Bacteriol 122, 826–831.
Vandewalle J, Bauters M, Van Esch H, Belet S, Verbeeck J, Fieremans N, Holvoet M, Vento J, Spreiz A, Kotzot D, Haberlandt E, *et al*. (2013). The mitochondrial solute carrier SLC25A5 at Xq24 is a novel candidate gene for non-syndromic intellectual disability. Hum Genet 132, 1177–1185.
Wach A, Brachat A, Pöhlmann R, Philippsen P (1994). New heterologous modules for classical or PCR-based gene disruptions in *Saccharomyces cerevisiae*. Yeast 10, 1793–1808.
Wang X, Salinas K, Zuo X, Kucejova B, Chen XJ (2008). Dominant membrane uncoupling by mutant adenine nucleotide translocase in mitochondrial diseases. Hum Mol Genet 17, 4036–4044.
Whited K, Baile MG, Currier P, Claypool SM (2013). Seven functional classes of Barth syndrome mutation. Hum Mol Genet 22, 483–492.
Wohlrab H, Flowers N (1982). pH gradient-dependent phosphate transport catalyzed by the purified mitochondrial phosphate transport protein. J Biol Chem 257, 28–31.
Wu M, Gu J, Guo R, Huang Y, Yang M (2016). Structure of mammalian respiratory supercomplex I1III2IV1. Cell 167, 1598–1609.